AD_____

Grant Number DAMD17-94-J-4117

TITLE: Role of Accessory Molecular in Endotoxin-Endothellial Interactions and Endothelial Barrier Dysfunction

PRINCIPAL INVESTIGATOR: Simeon E. Goldblum, M.D.

CONTRACTING ORGANIZATION: University of Maryland
School of Medicine
Baltimore, Maryland 21201

REPORT DATE: June 1998

TYPE OF REPORT: Final

PREPARED FOR: U.S. Army Medical Research and Materiel Command
Fort Detrick, Maryland 21702-5012

REPORT DOCUMENTATION PAGE

Form Approved
OMB No. 0704-0188

1. AGENCY USE ONLY *(Leave blank)*	2. REPORT DATE	3. REPORT TYPE AND DATES COVERED
	June 1998	Final (1 Jun 94 - 31 May 98)

4. TITLE AND SUBTITLE
Role of Accessory Molecular in Endotoxin-Endothellial Interactions and Endothelial Barrier Dysfunction

5. FUNDING NUMBERS
DAMD17-94-J-4117

6. AUTHOR(S)
Simeon E. Goldblum, M.D.

7. PERFORMING ORGANIZATION NAME(S) AND ADDRESS(ES)
University of Maryland
School of Medicine
Baltimore, Maryland 21201

8. PERFORMING ORGANIZATION REPORT NUMBER

9. SPONSORING/MONITORING AGENCY NAME(S) AND ADDRESS(ES)
U.S. Army Medical Research and Materiel Command
Fort Detrick, Maryland 21702-5012

10. SPONSORING/MONITORING AGENCY REPORT NUMBER

11. SUPPLEMENTARY NOTES

12a. DISTRIBUTION / AVAILABILITY STATEMENT
Approved for public release; distribution unlimited

12b. DISTRIBUTION CODE

13. ABSTRACT *(Maximum 200*

Bacterial lipopolysaccharide (LPS) is a component of Gram-negative bacteria known to induce actin reorganization, opening of the paracelluar pathway and loss of endothelial barrier function. We used an in vitro experimental system in which LPS derived from Escherichia coli O111:B4 was presented to postconfluent bovine pulmonary artery endothelial cell (EC) monolayers cultured on filter supports mounted in chemotaxis chambers. Transendothelial flux of 14C-bovine serum albumin was used as a quantitative measurement of paracellular permeability. We studied the roles of protein tyrosine phosphorylation and apoptosis in LPS-induced opening of the paracellular pathway and established that the lipid A moiety was the active portion of the LPS molecule in the non CD14-bearing EC system.

14. SUBJECT TERMS
Endothelium, barrier function, endotoxin, tyrosine phosphorylation, actin cytoskeleton, adherens junction, zonula adherens focal adhesions, caspases, apoptosis.

15. NUMBER OF PAGES
74

16. PRICE CODE

17. SECURITY CLASSIFICATION OF REPORT	18. SECURITY CLASSIFICATION OF THIS PAGE	19. SECURITY CLASSIFICATION OF ABSTRACT	20. LIMITATION OF ABSTRACT
Unclassified	Unclassified	Unclassified	Unlimited

FOREWORD

Opinions, interpretations, conclusions and recommendations are those of the author and are not necessarily endorsed by the U.S. Army.

SEG Where copyrighted material is quoted, permission has been obtained to use such material.

NA Where material from documents designated for limited distribution is quoted, permission has been obtained to use the material.

SEG Citations of commercial organizations and trade names in this report do not constitute an official Department of Army endorsement or approval of the products or services of these organizations.

NA In conducting research using animals, the investigator(s) adhered to the "Guide for the Care and Use of Laboratory Animals," prepared by the Committee on Care and use of Laboratory Animals of the Institute of Laboratory Resources, national Research Council (NIH Publication No. 86-23, Revised 1985).

NA For the protection of human subjects, the investigator(s) adhered to policies of applicable Federal Law 45 CFR 46.

NA In conducting research utilizing recombinant DNA technology, the investigator(s) adhered to current guidelines promulgated by the National Institutes of Health.

NA In the conduct of research utilizing recombinant DNA, the investigator(s) adhered to the NIH Guidelines for Research Involving Recombinant DNA Molecules.

NA In the conduct of research involving hazardous organisms, the investigator(s) adhered to the CDC-NIH Guide for Biosafety in Microbiological and Biomedical Laboratories.

Simeon E Goldblum 12/11/98

PI - Signature Date

(4) TABLE OF CONTENTS

(5) INTRODUCTION:

The mortality associated with Gram-negative bacteremia has not decreased despite improved antibiotic therapy. Complications resulting from these infections include: profound shock, disseminated intravascular coagulation, and vascular leak syndromes, including the acute respiratory distress syndrome (1). A common denominator to all of these complications is endothelial cell (EC) injury and dysfunction. Bacterial endotoxin or lipopolysaccharide (LPS), a component of the envelope of Gram-negative organisms, has been shown to directly provoke the EC injury associated with Gram-negative sepsis (2). Data that exists to support LPS as a key mediator of EC injury include: 1) administration of LPS to experimental animals reproduces the EC injury seen in animals challenged with Gram-negative bacteria (2), 2) LPS plasma levels correlate with the development of septic shock and multiorgan failure (3), and 3) in some experiments, interventions which specifically target the LPS molecule protect against the EC complications often associated with Gram-negative sepsis (4,5).

LPS directly induces pulmonary vascular EC injury *in vitro* in the absence of nonendothelial-derived host mediators (6,7). EC responses to LPS include: F-actin depolymerization and microfilament redistribution, changes in cell morphology, intercellular gap formation, and increased monolayer permeability (6,7).

The state of assembly and organization of the actin cytoskeletal network is closely linked to changes in EC monolayer permeability (7-10). Adherens junctions, which are responsible for cell-cell [zonula adherens (ZA)] and cell-substrate [focal adhesions (FA)] adhesion, are coupled to the actin cytoskeleton and play a key role in maintaining functional integrity of the EC barrier. It has been suggested that tyrosine phosphorylation events which compromise monolayer barrier function also mediate cytoskeletal reorganization and the disassembly of adherens junctions (11).

The presentation of LPS to CD14 bearing cells such as macrophages and monocytes has been

well characterized. LPS binds with the acute phase protein LPS-binding protein and the resulting complex recognizes membrane bound CD14 (12). CD14, a glycosylphosphatidyl inositol-anchored protein, has not been coupled to intracellular signal transduction, yet rapid tyrosine phosphorylation occurs after binding of LPS to CD14 (12). Even less is known about the interactions of LPS with non-CD14 bearing host cells such as the EC. Recently, tyrosine phosphorylation of mitogen-activated protein kinases has been demonstrated in LPS-stimulated EC (13). Furthermore, PTK inhibition has been shown to attenuate LPS-induced EC toxicity and interleukin-6 (IL-6) release *in vitro* (13), and to prevent LPS-induced lethality in mice (14).

Most bactericidal antibiotics that target viable, replicating Gram-negative bacteria do not diminish LPS activity and can actually liberate free LPS into the circulation (15). One notable exception, polymyxin B (PMB) derived from the bacteria *Bacillus polymyxa* (16,17), can bind to the lipid A portion of LPS and neutralize it. In the past, however, PMB's nephrotoxic properties have severely limited its therapeutic application. Other naturally occurring proteins exist which also bind to and neutralize LPS, including: bactericidal/permeability-increasing protein (BPI) and cationic antimicrobial protein 18 found in polymorphonuclear leukocytes (18,19), high and low density lipoproteins (20,21), and the *Limulus* anti-LPS factor (LALF) found in the horseshoe crab, *Limulus polyphemus* (22). LALF is a 11.8 kDa protein isolated from the amebocyte, the single blood cell type found in the horseshoe crab (22). The amebocyte-derived LALF as well as its recombinant form, endotoxin neutralizing protein (ENP), each binds to and neutralizes LPS (22,23). The LPS-binding site is 32 to 50 amino acids in length and forms an amphipathic loop which binds to the lipid A portion of LPS (23-25). ENP or LALF neutralizes LPS bioactivity in the *Limulus* amebocyte lysate assay (23,26), prevents macrophage production of TNF *in vitro* (27), and protects against LPS challenge *in vivo* (26,28).

LPS has been shown to induce EC apoptosis both *in vivo* and *in vitro* (29-31). In LPS challenged mice, widespread EC apoptosis, an event which could only be partially blocked by recombinant tumor necrosis factor α (TNFα) binding protein, has been demonstrated (31). LPS also directly induces EC activation of caspases *in vitro,* in the absence of endogenous mediators derived from non-EC sources, including TNFα (32). Caspases, which are cysteine proteases activated during apoptosis, cleave a limited number of cell proteins including the adherens junction components, β-catenin, γ-catenin, and focal adhesion kinase FAK (33-37).

(6) BODY:

A. EXPERIMENTAL METHODS:

Reagents. LPS phenol-extracted from *Escherichia coli* serotype 0111:B4, *E.coli 055:B5, Klebsiella pneumoniae, Pseudomonas aeruginosa, Salmonella minnesota*, and *Serratia marcescens* (Sigma Chemical Co., St. Louis, MO) were suspended in PBS at 5 mg/ml and these stock solutions were stored at 4 °C. Lipid A from *E. coli* K12 (List Biol. Lab., Campbell, CA) was dissolved into chloroform (69%), methanol (27%), and water (4%), evaporated under nitrogen, and the dry residue resuspended in water. To prepare the O-polysaccharide fraction, *E.* coli 0111:B4 LPS was hydrolyzed at 100 °C for 2 h with 1% acetic acid, neutralized with 1.0 M NaOH and centrifuged. The supernate containing the O-polysaccharide was desalted on a Sephadex G-25 (Pharmacia Biotech, Piscataway, NJ) column using water as elutant and the fractions were tested for O-polysaccharide by the phenol sulfuric acid method of Dubois et al (38). The O-polysaccharide-positive fractions were pooled and lyophilized. ENP was a gift from the Associates of Cape Cod (Woods Hole, MA). ENP was reconstituted at 1 mg/ml in PBS, aliquotted, and stored at -20 °C. PMB sulfate was purchased from Sigma and was reconstituted at 25.8 mg/ml and stored at 4 °C. The caspase inhibitor peptide, z-VAD-

fmk (z-VAD) and the negative control peptide, z-FA-fmk, were purchased from Calbiochem-Novabiochem Corp., (La Jolla, CA). LPS phenol-extracted from *Escherichia coli* serotype 0111:B4, polymyxin B (PMB) sulfate, staphylococcal enterotoxin B (SEB), herbimycin A, and dimethyl sulfoxide (DMSO) were obtained from Sigma Chemical Co., (St. Louis, MO). Recombinant human TNFα (specific activity $\geq 2 \times 10^7$ U/mg) was purchased from Endogen, Inc., (Woburn, MA).

EC Culture. Bovine pulmonary artery EC (BPAEC), obtained from the American Type Culture Collection (Rockville, MD), were cultured at 37 °C under 5% CO_2 in Dulbecco's Modified Eagle's Medium (Sigma) enriched with 20% fetal bovine serum (FBS) (Hyclone Laboratories, Inc., Logan, UT), 5 mM L-glutamine, nonessential amino acids, and vitamins, in the presence of penicillin (50 u/ml) and streptomycin (50 mg/ml) (Sigma). The cells were washed and gently detached with a brief (1-2 min) trypsin (0.5 mg/ml) (Sigma) exposure with gentle agitation followed immediately by trypsin-neutralization with FBS-containing medium. The cells were counted and suspended in medium for immediate seeding of tissue culture dishes or barrier function assay chambers. Cultures were determined to be endothelial by uniform cobblestone morphology and by quantitative determination of angiotensin-converting enzyme activity with commercially available ^{3}H-benzoyl-Phe-Ala-Pro substrate (Ventrex Laboratories, Inc., Portland, ME) (7).

Immunoblotting for Phosphotyrosines. EC were seeded at a density of 1.5×10^6 cells/100 mm cell culture dish (Corning Inc., Corning, NY) and cultured for 72 h to confluence. EC were exposed to a range of LPS concentrations for varying exposure times. In certain experiments, LPS (100 ng/ml, 1 h) was introduced in combination with sodium orthovanadate (50, 100, 200, or 250 μM) to maximize the LPS-induced elevated expression of phosphotyrosine-containing proteins. In some experiments, herbimycin A (1 μM) or genistein (50 μg/ml) were introduced 16 h and 1h, respectively, prior to and throughout the 1 h study period. Following treatment, the cells were washed x2 with ice-cold PBS

containing 1 mM vanadate. The cells were then lysed for 15 min with ice-cold modified radioimmunoprecipitation assay (RIPA) lysis buffer [50 mM Tris-HCl (pH 8.0), 1% Nonidet P-40, 0.25% sodium deoxycholate, 150 mM NaCl, 1 mM ethylene glycol tetraacetic acid (EGTA), 1 mM phenylmethylsulfonyl fluoride (PMSF), 1 μg/ml leupeptin, 1 μg/ml pepstatin, 1 μg/ml aprotinin, 1 μg/ml type 1 DNAse, 1 mM sodium orthovanadate, 1 mM NaF, 1 mM pyrophosphate, 1 mM phenylarsine oxide (PAO), 500 μM P-nitrophenyl phosphate, 1 mM dithiothreitol (DTT)]. The cells were scraped and transferred to a tube and centrifuged (16,000 g, 10 min, 4 °C). The supernatant was lyophilized and reconstituted in 500 μl of distilled water. The EC lysates (25 μg protein/lane) were resolved by SDS-PAGE on an 8-16% Tris-Glycine gradient gel (Novex Inc., San Diego, CA) and subsequently transferred for 3 h at 30 v to polyvinylidene fluoride membrane (PVDF). The membrane was blocked with 3% dry milk in PBS for 1 h at room temperature followed by incubation with biotinylated 4G10 anti-phosphotyrosine antibodies (0.7 μg/ml) (Upstate Biotechnology Inc., Lake Placid, NY) for 1 h. The blot was washed x2 with PBS, incubated with horseradish peroxidase (HRP)-conjugated streptavidin (0.5 μg/ml) (Upstate Biotechnology Inc.) for 0.5 h, and rinsed with 0.05% Tween in PBS followed by rinses with PBS x4. The blot was developed with enhanced chemiluminescence (Amersham Life Sciences, Arlington Heights, IL) and exposed to Du Pont Reflection (NEF-406) film. To insure equal protein loading, duplicate gels were stained with Coomassie Blue and subjected to laser densitometry.

Assay of Transendothelial Albumin Flux. Transendothelial ^{14}C-bovine serum albumin (BSA) flux was assayed as previously described (6,7). Briefly, polycarbonate filters (13 mm diameter, 0.4 μm pore size) (Nuclepore Inc., Pleasanton, CA) impregnated with pigskin gelatin (Fisher Scientific, Pittsburgh, PA) were mounted to polystyrene chemotactic chambers (ADAPS, Inc., Dedham, MA), and inserted into wells of 24-well plates. Each upper compartment was seeded with 2 x 10^5 EC and cultured for 72h (37 °C, 5% CO_2). We used ^{14}C-BSA (Sigma) with a specific activity of 30.1 mCi per mg protein as the tracer

molecule. The baseline barrier function of each monolayer was determined by applying ^{14}C-BSA (1.1 pmol/0.5 ml) to each upper compartment for 1h at 37 °C, after which the lower compartment was sampled and counted in a liquid scintillation analyzer (Packard Instruments Co., Grove, IL). Only endothelial monolayers retaining ≥95% of the ^{14}C-BSA were studied. The monolayers were then treated for 6 h with LPS (10 or 100 ng/ml), genistein (50 μg/ml), herbimycin A (1 μM), PAO (0.1 μM), vanadate (2.5 μM), or combinations of LPS and any one of the other agents. Genistein, herbimycin A, and PAO all required solubilization in DMSO. All inhibitors were simultaneously administered with LPS except for herbimycin A and genistein which were introduced 16 h and 0.5 h respectively, prior to LPS treatment. Dose response relationships were established for each pharmacological agent in the barrier function assay. The maximal subthreshold concentration for each agent was chosen. Transfer of ^{14}C-BSA across EC monolayers was again assayed. Simultaneous controls with either medium or DMSO-containing medium were also performed.

F-Actin Epifluorescence Microscopy. To maintain EC monolayers under identical experimental conditions to our permeability assay, we used a previously described method to directly stain and visualize the monolayers on polycarbonate filters (7). EC cultured to confluence on filters were exposed for 6 h to media alone, LPS (100 ng/ml), herbimycin A (1 μM), or LPS and herbimycin A. Herbimycin A was introduced 16 h prior to the study period. The monolayers were fixed (3.7 % formaldehyde, 20 min), permeabilized (0.5% Triton X-100 in HEPES buffer, 5 min), and stained with fluorescein-phalloidin (1.65 x 10^{-7} M, 20 min)(Molecular Probes). The filters and their attached monolayers were mounted cell-side up on microscope slides and photographed through a Zeiss Axioscop 20 microscope (100x oil, Plan Neofluar objective) equipped for epifluorescence.

G-Actin Quantitation. EC G-actin was measured using the DNAse 1 inhibition assay as previously described (7). The assay is based upon the ability of monomeric G-actin to inhibit DNAse hydrolysis of

type 1 DNA into its component nucleotides. DNAse 1 obtained from bovine pancreas (Sigma, St. Louis, MO) was mixed with calf thymus type 1 DNA substrate (Sigma) and the slope of the linear portion of the ΔA 260 recorded. Purified bovine skeletal muscle actin (Sigma) was used to create a standard curve for the standardization of the G-actin assay. EC monolayers were seeded in 6-well culture plates at a density of 3.8×10^5 cells/well and cultured 72 h to confluence. EC were exposed to media, herbimycin A, genistein, vanadate, PAO, or any combination of LPS and the preceding agents under similar conditions used to assay transendothelial albumin flux. Following treatment, monolayers were washed and permeabilized with a buffer containing 1% Triton X-100. The G-actin containing supernatants were then tested in the DNAse 1 inhibition assay to generate inhibitory activities that fell between 30 - 70 % inhibition, the range within which DNAse 1 inhibitory activity is directly proportional to monomeric G-actin. The inhibitory activities were interpolated to G-actin concentrations from the simultaneously run standard curve and expressed in microgram per milligram of total EC protein. Total EC protein was determined with the standard Bio-Rad DC Protein Assay (Bio-Rad Chemical Division, Richmond, CA) in simultaneously cultured monolayers subjected to conditions identical to those used in the G- and F-actin assays. Total EC protein was used to standardize both G- and F-actin measurements.

F-Actin Quantitation. Endothelial F-actin was fluorimetrically measured as previously described (7). EC (3.8×10^5 cells in 2 ml media) were seeded into the wells of 6-well plates and cultured for 72 h (37 °C, 5% CO_2). The monolayers were exposed to conditions identical to those used for the G-actin assay except that all of the monolayers were treated with 50 μg/ml cycloheximide for 30 min prior to and throughout the various treatment exposures as previously described (7). The monolayers were washed, fixed (3.7% formaldehyde, 15 min), permeabilized (0.2% Triton X-100, 5 min), stained with NBD-phallacidin (1 unit/well, 30 min) (Molecular Probes, Eugene, OR), and extracted with methanol (overnight, -20 °C). Fluorescence of each extract was measured in a Perkin-Elmer LS30 luminescence

spectrometer at 465 nm excitation (10 nm slit) and 535 nm emission (10 nm slit) and was expressed in arbitrary fluorescence units per mg total EC protein.

Phosphotyrosine Immunolocalization. As with the F-actin epifluorescence microscopy, EC monolayers were seeded under identical conditions to those of the barrier function assay. EC were treated with media or LPS (100 ng/ml) for 1 h and washed 3x with ice cold PBS containing 1 mM vanadate. Cells were fixed for 20 min in 4% formaldehyde in PBS at room temperature, washed twice with PBS, exposed to ice cold methanol for 6 min at -20 °C, and then incubated overnight with 1% BSA-PBS solution at 4 °C. EC were subsequently exposed to 5 μg/ml of FITC-conjugated anti-phosphotyrosine (Upstate Biotechnology Inc.) for 1 h at room temperature in the dark. Monolayers were washed twice with 1% PBS-BSA followed by x3 washes with PBS. The filters were removed from the chambers, mounted cell-side up on microscope slides and visualized through a Zeiss Axioscop 20 microscope (100x oil, Plan Neofluar objective).

Immunoprecipitation of Phosphotyrosine-Containing Proteins. LPS-exposed (100 ng/ml, 1 h) EC were lysed with modified RIPA buffer and the lysates incubated overnight with either of two murine monoclonal antibodies, PY20 anti-phosphotyrosine antibody (5 μg/ml) or anti-paxillin antibody (0.25 μg/ml) (both purchased from Transduction Laboratories, Lexington, KY) at 4 °C. The resultant immune complexes were immobilized by incubation with anti-mouse IgG cross-linked to agarose (Sigma) for 2 h at 4 °C and centrifuged. The pellet was washed x3 with modified RIPA buffer and boiled in sample buffer for 5 min. Proteins were resolved with SDS-PAGE and transferred onto PVDF as described above. Select lanes of the blot were subsequently probed with the anti-paxillin antibody (0.025 μg/ml) followed by incubation with HRP-conjugated anti-mouse IgG (0.13 μg/ml) (Transduction Laboratories). Other lanes of the blot were probed with biotinylated anti-phosphotyrosine (4G10) antibody (Upstate Biotechnology Inc.) as described above. In selected experiments, paxillin was immunoprecipitated from

lysates derived from LPS-exposed EC, and the paxillin-depleted supernatant resolved by SDS-PAGE, transferred to PVDF, and the blots probed with anti-phosphotyrosine (4G10) antibodies as described above. All lanes were then developed with enhanced chemiluminescence (Amersham Life Sciences).

Phosphotyrosine Colocalization with Paxillin. EC monolayers were seeded under identical conditions to those of the barrier function assay and treated for 1 h with media alone or LPS (100 ng/ml). Monolayers were washed, fixed, and permeabilized under conditions identical to those for immunolocalization as described above, with the exception that 0.5% Triton X-100 in PBS was used to permeabilize the cells instead of ice cold methanol. Permeabilized EC were exposed to mouse anti-paxillin antibody (5 μg/ml) for 1 h, washed x3 with 1% BSA in PBS, and then incubated with Texas Red-conjugated sheep anti-mouse IgG (3 μg/ml) (Cappel/Organon Teknika Corp., Durham, NC). After vigorous washing, the monolayers were then exposed to FITC-conjugated anti-phosphotyrosine (4G10) antibody and subsequently visualized as described above.

Filter Detachment Assay. Gelatin-impregnated polycarbonate filters (25 mm diameter, 0.4 mm pore size) (Nuclepore) were mounted in chemotactic chambers (ADAPS) which were inserted into the wells of 6-well plates. The chambers were seeded with 3.5×10^5 EC and cultured for 72 h. Following treatment, the supernatant and one wash from each well were pooled and the cells counted in triplicate. The remaining monolayer was trypsin-detached (0.5 mg/ml, 15 min) and the cells counted. Filters were stained with Coomassie brilliant blue to document complete cell detachment. Percent detachment was expressed as [total cells in the supernatant and wash] / [total cells in supernatant, wash, and detached from filter] x 100%.

Immunoblotting of Adherens Junction Proteins. Confluent EC monolayers were washed with ice-cold PBS containing 1 mM sodium orthovanadate, lysed with ice-cold modified radioimmunoprecipitation assay (RIPA) lysis buffer [50 mM Tris-HCl (pH 7.4), 1% Nonidet P-40, 0.25% sodium deoxycholate, 150

mM NaCl, 1 mM ethylenediaminetetra-acetic acid, protease inhibitor cocktail tablet (Boehringer Mannheim Corp., Indianapolis, IN), 1 μg/ml pepstatin, 1 μg/ml type 1 DNAse, 1 mM vanadate, 50 mM NaF], scraped, transferred to microcentrifuge tubes, and centrifuged (16,000 *g*, 10 min, 4°C). The supernatants (20 μg protein/lane) were resolved by SDS-PAGE on an 8-16% Tris-Glycine gradient gel (Novex Inc., San Diego, CA) and transferred to polyvinylidene fluoride (PVDF) membrane (Millipore Corp, Bedford, MA). Blots were blocked with 3% dry milk and then incubated with anti-α-catenin (1.0 μg/ml), anti-β-catenin (0.5 μg/ml), anti-γ-catenin (0.13 μg/ml), anti-focal adhesion kinase (FAK) (0.25 μg/ml), anti-$p120^{Cas}$ (0.3 μg/ml), anti-$p130^{Cas}$ (0.25 μg/ml) (all purchased from Transduction Laboratories Inc., Lexington, KY), anti-β-catenin NH_2-terminus (1:5000 dilution; generous gift of Dr. Barry M. Gumbiner of the Memorial Sloan-Kettering Cancer Center), or anti-pan cadherin (6.6 μg/ml; Sigma) antibodies for 1 h. The blots were incubated with horseradish-peroxidase (HRP)-conjugated anti-mouse or anti-rabbit immunoglobulin G (IgG) (0.13 μg/ml; Transduction Labs), developed with enhanced chemiluminescence (Amersham Life Sciences, Arlington Heights, IL), and exposed to Kodak X-Omat Blue film (NEN Life Sciences, Inc., Boston, MA). To insure equal protein loading, the blots were stained with Fast Green (Sigma) and then stripped with 100 mM 2-mercaptoethanol, 2% sodium dodecyl sulphate, 62.5 mM Tris-HCl, pH 6.7 at 70 ^{0}C for 30 min, washed, blocked, and reprobed with anti-β-tubulin murine monoclonal antibody (0.5 μg/ml; Boehringer Mannheim) followed by HRP-conjugated anti-mouse IgG (0.13 μg/ml) (Transduction Labs).

Immunoprecipitation (IP) of Adherens Junction Proteins. EC were lysed with modified RIPA buffer and the lysates incubated overnight at 4 °C with anti-pan cadherin, anti-α-catenin, anti-APC (Santa Cruz Biotechnology, Inc., Santa Cruz, CA), or anti-paxillin antibodies (2.5 μg of antibody/500 μg total protein). The resultant immune complexes were immobilized by incubation with either anti-mouse or anti-rabbit IgG cross-linked to agarose (Sigma) for 2 h at 4 °C and centrifuged. The pellet was washed

three times with modified RIPA buffer, boiled in 2x sample buffer [5x sample buffer: 62.5 mM tris-HCl (pH 6.8), 2.5% SDS, 25% glycerol, 1% 2-beta-mercaptoethanol, and 0.1% bromophenol blue], and immunoblotted as described above. In other experiments, blots of EC paxillin immunoprecipitates were incubated for 1 h with a biotinylated 4G10 anti-phosphotyrosine antibody (0.7 μg/ml; Upstate Biotechnology Inc., Lake Placid, NY) followed by HRP-conjugated streptavidin (0.5 μg/ml; Upstate Biotechnology). To monitor efficiency of IP and protein loading, blots containing paxillin immunoprecipitates were stripped and reprobed with anti-paxillin antibody (0.025 μg/ml; Transduction Labs). The blots were analyzed by laser densitometry (Molecular Dynamics Corp., Sunnyvale, CA) and the phosphotyrosine signal normalized to paxillin. The relative amount of paxillin tyrosine phosphorylation following LPS exposure was expressed relative to the simultaneous medium controls. For those monolayers exposed to LPS (100 ng/ml; 6 h) in the presence of the z-VAD caspase inhibitor, the relative amount of paxillin tyrosine phosphorylation was expressed relative to that detected in EC exposed to z-VAD alone.

Detection of Apoptosis. LPS-induced EC apoptosis was assayed by both DNA laddering and TUNEL (terminal deoxynucleotidyl transferase-mediated dUTP nick end labeling) assays (39). To assess DNA laddering, EC harvested with a cell scraper from treated monolayers were centrifuged (200 *g*, 5 min) and resuspended in 200 μl of PBS. DNA was isolated using the Apoptotic DNA Ladder kit (Boehringer Mannheim). Isolated DNA was incubated with RNase, DNase-free (2 μg/ml, 20 min, room temperature; Boehringer Mannheim) and 2 μg of DNA was resolved on a 2% agarose gel containing 0.5 μg/ml of ethidium bromide. DNA in the gel was visualized by ultraviolet (UV) light and photographed with Polaroid positive/negative film (Polaroid Corp., Cambridge, MA).

For the TUNEL assay, EC cultured in the wells of chamber slides (Nalge Nunc International Corp., Naperville, IL) were treated, fixed in 4% paraformaldehyde, and permeabilized (0.1% Triton X-

100, 0.1% sodium citrate; 3 min at 4 °C). Each well was exposed to 100 µl of TUNEL reaction mixture (Boehringer Mannheim) in a humidified chamber for 1 h at 37 °C in the dark. The slides were rinsed and mounted with anti-fade mounting medium (Vector Laboratories Inc., Burlingame CA) under glass coverslips. The monolayers were photographed through a Zeiss Axioscop 20 microscope (100x oil, 1.3 N.A., Plan Neofluar objective). For phase contrast microscopy, EC were visualized through a Zeiss inverted microscope (10x, .25 N.A., F-Achromat PH1 objective).

Statistical Methods. For time-dependent measurements (transendothelial albumin flux, filter detachment assays, and relative state of paxillin tyrosine phosphorylation), the mean response for each experimental group was compared with its respective control utilizing the Student's *t* test. For other measurements, analyses of variance (ANOVA) was used to compare the mean responses among experimental and control groups. In various studies, the Scheffe F-test, Bonferroni post hoc comparison test, or Tukey *post-hoc* comparison test was used to determine between which groups significant differences existed. For all statistical methods employed, a p-value of <0.05 was considered significant.

B. RESULTS:

Dose- and time-dependent effect of LPS on protein tyrosine phosphorylation. EC lysates from LPS-exposed cells revealed an increase in tyrosine phosphorylation of a protein of apparent molecular weight of 65 kDa (Fig. 1). Duplicate gels ran simultaneously were stained with Coomassie Blue; no differences in protein loading were detected. The increased state of protein tyrosine phosphorylation was seen at LPS concentrations of $\geq$ 10 ng/ml after which the level of tyrosine phosphorylation appeared to plateau (Fig. 1A). A dose-dependent shift in the mobility of this band was detected, which is characteristic of tyrosine phosphorylated proteins. EC monolayers were then exposed to a fixed LPS concentration (100 ng/ml) for increasing exposure times (Fig. 1B). LPS increased the 65 kDa phosphotyrosine-containing band as early as 30 min, and at 60 min this increase was maximal ($p< 0.02$). At 2 h, the difference in levels of tyrosine

phosphorylation between EC exposed to LPS or media alone was diminished and by 4h, this difference was undetectable. In order to maximize LPS-induced protein tyrosine phosphorylation, EC were exposed to LPS (100 ng/ml, 1h) or media, each in the presence of increasing concentrations of vanadate, a protein tyrosine phosphatase (PTP) inhibitor (Fig. 1C). In the presence of PTP inhibition, protein tyrosine phosphorylation in LPS-exposed EC was increased relative to that seen after exposure to either vanadate controls or LPS alone. The enhanced signal resulting from vanadate exposure did not increase the relative difference in tyrosine phosphorylation between LPS- and media-exposed EC. In many experiments, increased phosphotyrosine signal in a band with apparent molecular weight of 130 kDa was also evident. This increase in tyrosine phosphorylation appeared to mirror the increased phosphotyrosine signal for the 65 kDa band. Unlike the changes in the 65 kDa band, the changes for the 130 kDa band were not demonstrable in all experiments. No further efforts were made to identify this protein.

Effects of PTK inhibitors on LPS-induced increases in transendothelial ^{14}C-BSA flux. The mean (± SE) pretreatment baseline ^{14}C-BSA flux across monolayers was 0.012 pmol/h (± 0.001) (n = 93) (Fig. 2A). LPS exposure (100 ng/ml, 6 h) resulted in an ~ two-fold increase in transendothelial flux compared to media controls. The introduction of herbimycin A (1 μM) or genistein (50 μg/ml) in combination with LPS resulted in 100% and 77% protection against the LPS-induced increment in flux, respectively. Transendothelial ^{14}C-BSA flux across EC exposed to either one of these functionally and structurally dissimilar PTK inhibitors alone did not significantly differ from the albumin flux across media control monolayers.

Effect of PTK inhibitors on LPS-induced protein tyrosine phosphorylation. The ability of herbimycin A and genistein to each specifically inhibit tyrosine phosphorylation of the 65 kDa protein in response to LPS was studied (Fig. 2B). Phosphotyrosine immunoblotting of lysates from EC exposed to LPS in the presence and absence of PTK inhibitors was performed (Fig. 2B). Either herbimycin A or

genistein protected against the LPS-induced increase in tyrosine phosphorylation of the 65 kDa.

Effect of PTK inhibition on LPS-induced intercellular gap formation. F-actin probed EC monolayers exposed for 6h to media alone (Fig. 3A), herbimycin A (1 μM) (Fig. 3B), LPS (100 ng/ml) (Fig. 3C), or LPS with herbimycin A (Fig. 3D) were photographed through an epifluorescence microscope. The medium control (Fig. 3A) and the monolayers exposed to herbimycin A alone (Fig. 3B) both exhibited tight cell-to-cell apposition without intercellular gaps. As expected, LPS-treated monolayers displayed intercellular gap formation (Fig. 3C). The introduction of herbimycin A protected against the formation of these intercellular gaps in response to LPS (Fig. 3D).

Effect of PTK inhibition on LPS-induced increments in the EC G-actin pool. The G-actin pools were studied in EC exposed for 6 h to media alone, herbimycin A (1μM), genistein (50 μg/ml), LPS (100 ng/ml), LPS with herbimycin A, or LPS with genistein (Fig. 4A). The G-actin pools in EC exposed to either herbimycin A or genistein were not different from their respective media controls. LPS increased the G-actin pool compared to simultaneous media controls and this increase could be diminished by either herbimycin A or genistein. In fact, when LPS was coadministered with genistein, the G-actin pool was not significantly greater than the simultaneous media control.

Effect of PTK inhibition on LPS-induced decrements in the EC F-actin pool. The effect of PTK inhibition on LPS-induced decrements of the F-actin pool were studied (Fig. 4B). F-actin in EC exposed to either herbimycin A or genistein was not different from respective media controls. Monolayers treated with LPS (100 ng/ml, 6 h) had significantly decreased F-actin compared to their simultaneous media controls (Fig. 4B). PTK inhibition with either herbimycin A or genistein protected against the LPS-induced F-actin decrement. In fact, EC exposed to LPS in the presence of herbimycin A were not significantly different than either the simultaneous media or herbimycin A controls.

Effects of PTP inhibition on LPS-induced increases in transendothelial ^{14}C-BSA flux. Since PTK

inhibition blocked monolayer disruption by LPS, we studied whether PTP inhibition enhanced the LPS effect (Fig. 5). Exposure to vanadate or PAO alone did not alter albumin flux compared to their respective media controls. Coadministration of either vanadate (2.5 μM) or PAO (0.1 μM) with LPS (10 ng/ml, 6 h) significantly enhanced the LPS-induced increment in transendothelial flux of ^{14}C-BSA compared to monolayers exposed to LPS alone.

Effect of PTP inhibition on LPS-induced increases of the EC G-actin pool. After finding that PTP inhibition could enhance the LPS-induced permeability of EC monolayers, we examined whether vanadate (2.5 μM) or PAO (0.1 μM) could enhance the G-actin increase that results from LPS treatment. Monolayers exposed to vanadate or PAO alone did not demonstrate differences in G-actin relative to their media controls. The introduction of either inhibitor in combination with LPS (10 ng/ml, 6 h) increased the G-actin pool compared to LPS treatment alone (Fig. 6).

Immunolocalization of phosphotyrosine-containing proteins. EC monolayers were exposed for 1 h to media or LPS (100 ng/ml), probed for phosphotyrosine-containing proteins, and visualized through an epifluorescence microscope (Fig. 7). After LPS treatment, phosphotyrosine-containing proteins were localized to the intercellular boundaries in LPS-exposed monolayers (Fig. 7B). LPS treated-monolayers also displayed phosphotyrosine-containing plaque-like structures resembling FAs.

Identification of Paxillin as the 65 kDa Phosphotyrosine-Containing Protein. The 65 kDa tyrosine-phosphorylated protein and paxillin immunoprecipitated from LPS-exposed EC, comigrated to the same position on the blot (Fig. 8A). The 50 kDa band seen in lanes blotted with anti-paxillin antibody is the IgG heavy chain from the immunoprecipitating antibody under denaturing conditions. After immunodepletion (ID) of paxillin, the 65 kDa tyrosine-phosphorylated band disappeared (Fig. 8B). The band was recovered in the paxillin immunoprecipitate (IP).

Colocalization of Phosphotyrosine-Containing Proteins and Paxillin. EC monolayers were exposed

to media (A-C) or LPS (100 ng/ml, 1 h) (D-F), and probed for both phosphotyrosine-containing proteins and paxillin (Fig. 9). The LPS-exposed EC demonstrated increased protein tyrosine phosphorylation (D) compared to media control monolayers (A). The tyrosine phosphorylated proteins displayed a plaque-like distribution and colocalized with paxillin (F). The relative abundance and distribution of paxillin was similar for both media- and LPS-exposed monolayers (B,E).

Structure-function studies of LPS-induced endothelial barrier dysfunction. The mean ($\pm$ SE) pretreatment baselines reflecting functional integrity for monolayers to be exposed to either lipid A or the O-specific polysaccharide fraction were 0.016 $\pm$ 0.002 pmol/h and 0.013 $\pm$ 0.002, respectively (Figure 10A). The mean ($\pm$ SE) ^{14}C-BSA flux across naked filters without endothelial monolayers was 0.215 $\pm$ 0.015 pmol/h. Increasing concentrations of lipid A caused dose-dependent increases in ^{14}C-BSA flux across endothelial monolayers whereas identical concentrations of the O-specific polysaccharide fraction did not (Figure 10A). The lowest lipid A concentration that after a 6 h exposure increased ^{14}C-BSA flux compared to the simultaneous medium control was 15 ng/ml. Further dose-dependent increments were evident at concentrations up to 15 μg/ml. The polysaccharide fraction at concentrations up to 15 μg/ml failed to increase ^{14}C-BSA compared to the simultaneous media control.

PMB binds to and neutralizes the lipid A moiety of LPS. To determine whether lipid A was essential for LPS presentation to the nonCD14-bearing EC, the ability of PMB to block native LPS-induced barrier dysfunction was also studied (Figure 10B). ^{14}C-BSA flux was assayed immediately after 6 h exposures to medium, LPS (10 ng/ml), PMB (10 μg/ml), or LPS coadministered with increasing concentrations of PMB (10-10,000 ng/ml). LPS increased ^{14}C-BSA flux compared to the simultaneous medium control, whereas PMB alone did not. PMB at a PMB:LPS dry weight-to-weight ratio of 1:1 did not significantly diminish the LPS effect. At PMB concentrations of $\geq$ 1,000 ng/ml

(PMB:LPS dry weight-to-weight ratio of 100:1), PMB completely protected against the LPS effect, returning barrier function to medium control levels.

Effect of ENP on LPS-induced changes in transendothelial ^{14}C-BSA flux. ENP protected against LPS-induced barrier dysfunction (Figure 11). ^{14}C-BSA flux was assayed immediately after 6 h exposures to medium, LPS (10 ng/ml), ENP (10 μg/ml), or LPS coadministered with increasing concentrations of ENP (10-10,000 ng/ml). Again, LPS alone (10 ng/ml) increased ^{14}C-BSA flux compared to the simultaneous medium control. Protection against LPS-induced increases in ^{14}C-BSA flux by coadministration of ENP was dose-dependent. ENP $\geq$ 10 ng/ml significantly decreased LPS-induced barrier dysfunction. Partial protection was seen at an ENP concentration of 10 ng/ml (ENP:LPS dry weight-to-weight ratio of 1:1). Total protection was seen with ENP concentrations of $\geq$100 ng/ml (ENP:LPS ratio of $\geq$ 10:1). When ENP was introduced prior to a 5 min LPS challenge for either 0.5 h or 1.0 h and subsequently removed by thorough washing, no protection was observed (Table 1). Similarly, if ENP was introduced immediately following the LPS, again, no protection could be demonstrated.

A comparison of the protective effects of PMB (MW = 1,450 g/mol) and ENP (MW = 12,189 g/mol) suggests that ENP is more effective at blocking LPS-induced loss of EC barrier function. Complete protection against LPS (10 ng/ml)-induced transendothelial ^{14}C-albumin flux was observed with either $\geq$ 6.90 x 10^{-7} M PMB (PMB:LPS dry weight-to-weight ratio of $\geq$ 100:1) or $\geq$ 8.2 x 10^{-9} M ENP (ENP:LPS dry weight-to-weight ratio of $\geq$ 10:1). Partial protection was observed with $\geq$ 6.90 x 10^{-8} M PMB (PMB:LPS dry weight-to-weight ratio of $\geq$ 10:1) or 8.20 x 10^{-10} M ENP (ENP:LPS dry weight-to-weight ratio of $\geq$ 1:1).

Effect of ENP on LPS-induced tyrosine phosphorylation of EC proteins. Lysates obtained from EC exposed for 1 h to medium alone, ENP (1.0 μg/ml), LPS (100 ng/ml) or LPS coadministered with

ENP were resolved by SDS-PAGE, transferred to PVDF, and the blot probed for phosphotyrosines (Figure 12). Monolayers exposed to LPS demonstrated a 2.2 fold increase in tyrosine phosphorylation of a 66 kDa band compared to media alone; those monolayers exposed to LPS in the presence of ENP demonstrated only a 1.3 fold increase in tyrosine phosphorylation of this same 66 kDa protein. The increased tyrosine phosphorylation of this band in LPS-exposed EC relative to those exposed to media alone was inhibited by 75% when LPS was coadministered with ENP.

EC monolayers exposed for 1 h to medium, ENP (1.0 μg/ml), LPS (100 ng/ml), or LPS coadministered with ENP were probed with a FITC-conjugated anti-phosphotyrosine antibody, processed for epifluorescence microscopy, and photographed (Figure 13). At 1 h, LPS-exposed EC (Figure 13C) displayed increased tyrosine phosphorylation of proteins immunolocalized to the intercellular boundaries compared to both medium and ENP controls (Figures 13A and 13B, respectively). Monolayers treated with both ENP and LPS (Figure 13D) could not be distinguished from either the medium or ENP controls.

Effects of ENP on the LPS-induced changes in the F- and G-actin pools. The effect of ENP on the LPS-induced decrement in EC F-actin, expressed as fluorescence units/mg total EC protein, was studied (Figure 14A). There were no significant differences in F-actin content between the medium and ENP controls. A 6 h exposure to LPS (10 ng/ml) decreased F-actin compared to either simultaneous medium or ENP (100 ng/ml) controls. ENP coadministered with LPS diminished the LPS-induced F-actin decrement compared to LPS alone. In fact, F-actin content in EC treated with both LPS and ENP did not significantly differ from the simultaneous medium control.

The effect of ENP on the LPS-induced increment in EC G-actin, expressed in μg/mg total EC protein, was also studied (Figure 14B). A 6 h exposure to LPS (10 ng/ml) increased G-actin compared to either the simultaneous medium or ENP (100 ng/ml) controls. ENP coadministered with LPS

reduced the LPS-induced G-actin increment compared to that observed after exposure to LPS alone. This reduction was complete, reducing G-actin to the basal levels seen in the medium control. Therefore, LPS provokes reciprocal shifts between the F- and G-actin pools indicative of EC actin depolymerization and these changes are completely blocked by ENP.

ENP crossprotects against LPS derived from diverse Gram-negative bacterial strains. ENP offered protection against loss of barrier function in response to a variety of endotoxins normalized on the basis of KDO content to 10 ng/ml of LPS derived from *E. coli* O111:B4 (Figure 15). Monolayers were assayed for ^{14}C-BSA flux immediately after 6 h exposures to the following: medium, LPS derived from *E. coli* O111:B4, *E. coli* 055:B5, *K. pneumonia*, *P. aeruginosa*, *S. minnesota*, or *S. marcescens*, or an equivalent concentration of each LPS preparation coadministered with ENP (100 ng/ml). All LPS preparations except that derived from *S. marcescens*, induced comparable increments in ^{14}C-BSA flux. ENP completely protected against LPS-induced increments in ^{14}C-BSA transendothelial flux for all endotoxins tested.

Dose- and time-dependent effect of LPS on transendothelial ^{14}C-BSA flux and EC detachment. LPS exposure for 6 h increased transendothelial ^{14}C-BSA flux in a dose-dependent manner (Fig. 16A). The mean (± SE) pretreatment transendothelial ^{14}C-BSA flux was 0.017 ±0.001 pmol/h (n = 94) and the mean (± SE) ^{14}C-BSA transfer across naked filters without endothelial monolayers was 0.215 ± 0.015 pmol/h (n=16). LPS at concentrations ≥1 ng/ml increased ^{14}C-BSA flux compared to the simultaneous medium control. The LPS-induced effect appeared to plateau at concentrations of ≥100 ng/ml. The LPS effect on endothelial barrier function was also time-dependent (Fig. 16B). LPS exposures (10 ng/ml) of ≥2h increased ^{14}C-BSA flux compared to the simultaneous medium control. For the EC detachment studies, the mean (± SE) total cell counts (supernatant + wash + filter) from LPS-exposed monolayers and media controls were not significantly different at all time points tested. The mean (± SE) percent

detachment for cells exposed for 6 h to LPS ≥10 ng/ml was increased compared to the simultaneous medium controls (Fig. 16C); at 1 ng/ml the LPS effect approached but did not reach statistical significance ($p = 0.0748$). The mean (± SE) percent detachment of cells exposed to LPS 10 ng/ml was increased at ≥ 2 h compared to the simultaneous medium controls (Fig. 16D). Therefore, endothelial barrier dysfunction and EC detachment could be each induced by comparable LPS concentrations and exposure times.

Dose- and time-dependent effect of LPS-induced EC apoptosis. LPS exposure for 4 h induced apoptosis in a dose-dependent manner as assayed by DNA fragmentation into multiples of approximately 180 base pairs (bp) (Fig. 17A). DNA fragmentation was observed at LPS concentrations ≥1 ng/ml. The LPS-induced effect appeared to plateau at concentrations of ≥30 ng/ml. LPS-induced apoptosis was also time-dependent (Fig. 17B). DNA laddering was observed at LPS exposures (100 ng/ml) of ≥ 2 h.

Dose- and time-dependent effect of LPS-induced cleavage of ZA and FA component proteins. After establishing that LPS induces EC apoptosis and that the dose and time requirements for this event were compatible with those for EC barrier function and detachment, adherens junction proteins which mediate cell-cell and cell-substrate adhesion were studied. Western analysis of LPS-exposed EC revealed a dose- and time-dependent cleavage of the ZA proteins, β-catenin and γ-catenin (Fig. 18). The other components of the ZA, cadherin, α-catenin, and $p120^{Cas}$, remained intact. At concentrations ≥ 3 ng/ml, 6 h LPS exposures induced proteolysis of both β-catenin and γ-catenin (Fig. 18A). Further, LPS exposure (100 ng/ml) times of ≥ 2 h were required for the cleavage events (Fig. 18B). β-catenin cleavage generated a 70 kDa fragment; γ-catenin was cleaved into two distinct fragments of 74 and 64 kDa. The 74 kDA γ-catenin cleavage product appeared at lower LPS concentrations than the 64 kDa product. The FA proteins, FAK and $p130^{Cas}$, were similarly cleaved in a dose- (Fig. 19A) and time-dependent (Fig. 19B) manner. Proteolysis of FAK and $p130^{Cas}$ generated 96 kDa and 33 kDa cleavage products,

respectively. Two other FA proteins, paxillin and talin, remained intact and their relative abundance did not change (data not shown). The relative abundance of the cytoskeletal protein, β-tubulin, remained constant throughout the LPS exposure (Fig. 19A and B).

Caspase Inhibition Blocks LPS-Induced Protein Cleavage and Apoptosis. The caspase inhibitor peptide, z-VAD, was tested for its ability to block LPS-induced cleavage of adherens junction proteins. The peptide inhibited LPS-induced cleavage of β-catenin, γ-catenin, FAK, and $p130^{Cas}$ in a dose-dependent manner at concentrations of $\geq$ 12.5 μM; almost complete inhibition was seen with 100 μM z-VAD (Fig. 20A). The generation of the 64 kDa γ-catenin fragment was blocked at lower concentrations of the caspase inhibitor than the 74 kDa fragment. A negative control peptide (z-FA-fmk) which inhibits the cysteine protease, cathepsin B, failed to completely block LPS-induced cleavage of β-catenin and FAK. Although it appeared to block the generation of the 64 kDa fragment of γ-catenin, it had no inhibitory effect on the generation of the 74 kDa fragment. Since z-VAD could block LPS-induced protein cleavage, the ability of this peptide to block LPS-evoked apoptosis was assessed by two independent assays, DNA laddering (Fig. 20B) and TUNEL (Fig. 20C). LPS-induced (100 ng/ml, 4 h) EC DNA fragmentation was completely blocked by the z-VAD (100 μM) peptide (Fig. 20B). The ability of this peptide to inhibit LPS-induced apoptosis was confirmed by the TUNEL assay (Fig. 20C). Visualization with fluorescence microscopy of EC exposed to LPS (100 ng/ml, 4 h) revealed cells which were preferentially labeled with the fluorescent nucleotide (Fig. 20C iv-vi). The labeled chromatin in these cells was condensed and apoptotic bodies were evident. EC exposed to LPS in the presence of z-VAD (Fig. 20C iii), z-VAD alone (Fig. 20C ii), or medium (Fig. 20C i), displayed no fluorescent signal.

Effect of Caspase Inhibition on LPS-induced Disruption of the Endothelial Monolayer. Since caspase inhibition protected against LPS-induced cleavage of ZA proteins, the ability of z-VAD to block LPS-induced increments in ^{14}C-BSA was studied (Fig. 21). At concentrations which could block both

LPS-induced apoptosis and cleavage of FA and ZA proteins, the caspase inhibitor, z-VAD (100 μM), did not abrogate LPS-induced loss of barrier function. Since LPS-induced opening of the endothelial paracellular pathway can be blocked by protein tyrosine kinase (PTK) inhibition, we studied whether PTK inhibition with herbimycin A could also block LPS-induced cleavage events. Herbimycin A (1 μM) protected against LPS-induced increments in ^{14}C-BSA flux (Fig. 21), but did not block cleavage of adherens junction proteins (Fig. 21 insert).

Influence of β-Catenin Cleavage on Its Protein-Protein Interactions. As a first test as to whether β-catenin cleavage affected sequences that are established binding sites for β-catenin-binding proteins, antibodies raised against either the COOH-terminus (amino acids 571-781) or the NH_2-terminus (amino acids 6-138) were used to probe blots of lysates of EC exposed to LPS (100 ng/ml; 6 h) or medium alone (Fig. 22A). The antibody directed against the NH_2-terminus failed to recognize the 70 kDa fragment, localizing the cleavage site(s) to the NH_2-terminus. IP of α-catenin, which binds to the NH_2-terminus of β-catenin, or IP of cadherin or APC, both of which bind to the COOH-terminus of β-catenin, co-immunoprecipitated both the full-length and truncated forms of β-catenin (Fig. 22B).

Effect of Caspase Inhibition on LPS-Induced EC Detachment. Since caspase inhibition blocked cleavage of FA proteins, the ability of the caspase inhibitor peptide to block LPS-induced EC detachment was studied (Fig. 23). Introduction of z-VAD (100 μM) protected against LPS-induced (100 ng/ml; 4 h) EC detachment (Fig. 23A) as well as morphological changes associated with apoptosis (Fig. 23B). The PTK inhibitor, herbimycin A (1 μM), conferred only partial protection against LPS-induced detachment (Fig. 23A). EC exposed to LPS (100 ng/ml, 4 h) displayed widespread cell rounding and detachment from the underlying substrate (Fig. 23B v). These changes were diminished by the z-VAD peptide (100 μM) (Fig. 23B vi) and to a lesser extent by herbimycin A (1 μM) (Fig. 23B vii), but not by the negative control peptide, z-FA-fmk (100 μM) (Fig. 23B viii).

Influence of FAK Cleavage on Its Protein-Protein Interactions. FAK, a PTK localized to specialized areas of cell-substrate adhesion, binds to and tyrosine phosphorylates another FA protein, paxillin. IP of paxillin co-immunoprecipitated full-length FAK but not the cleavage product (Fig. 24A). The anti-FAK antibody which recognizes both the full-length FAK and its cleavage product, binds to the region of FAK (amino acids 354 - 533) which contains its catalytic domain. Paxillin binds to the COOH-terminus of FAK (amino acids 919 - 1042). These findings indicate that LPS-induced cleavage of FAK leads to the disassociation of paxillin from the kinase domain of FAK. We then wanted to determine whether this disassociation affected the tyrosine phosphorylation state of paxillin. In EC incubated with LPS (100 ng/ml) for increasing exposure times, tyrosine phosphorylation of paxillin decreased over time whereas in medium controls it remained constant (Fig. 24B). This LPS-induced decrease in tyrosine phosphorylation of paxillin was prevented by coadministration of the caspase inhibitor, z-VAD (100 μM) (Fig. 24C). LPS exposures of $\geq$ 4 h decreased tyrosine phosphorylation of paxillin compared to the simultaneous medium controls and at 6 h, the z-VAD peptide conferred ~ 90% protection against this decrease (Fig. 24D).

The Lipid A Portion of LPS Induces Cleavage of the ZA and FA Proteins. LPS, as the name implies, is composed of both lipid and polysaccharide components. We have previously demonstrated that the lipid A component of LPS is the bioactive portion responsible for inducing EC barrier dysfunction. To determine whether lipid A induces cleavage of adherens junction proteins, we coadministered LPS with either PMB or ENP, two structurally distinct proteins which bind to and neutralize lipid A (Fig. 25A). At concentrations which completely block LPS-induced increments in ^{14}C-BSA flux, ENP (1 μg/ml) and PMB (10 μg/ml) were able to protect against LPS-induced cleavage of ZA and FA component proteins (Fig. 25A).

SEB and TNFα also Induce Cleavage of ZA and FA Component Proteins. To determine whether cleavage of EC adherens junction proteins was specific to LPS, we incubated EC with concentrations of

either SEB (100 μg/ml) or TNFα (500 U/ml) which induce comparable barrier dysfunction to that seen with 100 ng/ml of LPS (Fig. 25B). Both agonists were able to induce identical cleavage of β-catenin and FAK (Fig. 25B). For a hypothetical schema see (Fig 26).

(7) **CONCLUSIONS**:

1. LPS induces tyrosine phosphorylation of an EC protein in a dose- and time- dependent manner. The phosphoprotein has a MW = 65kDa and has now been identified as the focal adhesion component, paxillin. This effect appears after an LPS exposure time of 0.5-1.0h to LPS concentrations of ≥ 10ng/ml.
2. The phosphotyrosine-containing proteins in LPS-exposed EC monolayers could be immunolocalized to the intercellular boundaries as well as to plaque-like structures.
3. The phosphotyrosine-containing proteins restricted to the plaque-like structures co-localized with paxillin.
4. Tyrosine kinase inhibition protects against: (a) LPS-induced EC actin depolymerization i.e. an increase in the G-actin pool with a reciprocal decrease in the F-actin pool, (b) LPS-induced intercellular gap formation, and (c) LPS-induced loss of endothelial barrier function.
5. In contrast, tyrosine phosphatase inhibition enhances: (a) LPS-induced EC actin depolymerization, and (b) LPS –induced loss of endothelial barrier function.
6. Endotoxin neutralizing protein (ENP) at an ENP:LPS ratio of 10:1 blocked LPS-induced tyrosine phosphorylation, actin depolymerization, intercellular gap formation, and loss of barrier function.
7. ENP cross-protects against loss of barrier function in response to LPS derived from diverse Gram -negative bacteria.

8. LPS induces dose- and time- dependent EC apoptosis with caspase activation and proteolytic cleavage of zonula adherens (β-and γ-catenins) and focal adhesion (FAK and $p130^{Cas}$) component proteins.
9. Caspase inhibition protects against LPS-induced EC apoptosis, proteolytic cleavage of adherens junction proteins, and EC detachment but not LPS-induced loss of endothelial barrier function.
10. LPS-induced cleavage of β-catenin did not disrupt its interactions with β-catenin-binding proteins including α-catenin and APC.
11. LPS-induced cleavage of FAK resulted in the disassociation of its catalytic domain from its substrate paxillin. This FAK-paxillin disengagement diminished the tyrosine phosphorylation state of paxillin
12. The lipid A portion of LPS induced the caspase mediated proteolysis of adherens junction proteins.
13. Another exogenous bacterial-derived stimulus, staphylococcus enterotoxin B, and the endogenous mediator, TNFα, each also induced cleavage of adherens junction proteins.

(8) REFERENCES

1. Danner, R.L., R.J. Elin, J.M. Hosseini, R.A. Wesley, J.M. Reilly, and J.E. Parillo. Endotoxemia in human septic shock. *Chest.* 99:169-175, 1991.
2. Brigham, K.L., and B. Meyrick. Endotoxin and lung injury. *Am. Rev. Respir. Dis.* 133:913-927, 1986.
3. Brandtzaeg, P., P. Kierulf, P. Gaustad, A. Skulberg, J.N. Bruun, S. Halvorsen, and E. Sorensen. Plasma endotoxin as a predictor of multiple organ failure and death in systemic meningococcal disease. *J. Infect. Dis.* 159:195-204, 1989.
4. Opal, S.M., C.J. Fisher, A.S. Cross, J.E. Palardy, D.L. Hoover, M.N. Marra, and R.W. Scott. Bactericidal/permeability-increasing protein as an anti-endotoxin therapeutic agent: comparisons with anti-core glycolipid polyclonal antibody therapy. *Clin. Res.* 40:213A, 1992.
5. Ziegler, E.J., J.A. McCutchan, J. Fierer, M.P. Glauser, J.C. Sadoff, H. Douglas, and A.I. Braude. Treatment of gram-negative bacteremia and shock with antiserum to a mutant *Escherichia coli. N. Eng. J. Med.* 307:1225-1230, 1982.
6. Goldblum, S.E., T.W. Brann, X. Ding, J. Pugin, and P.S. Tobias. Lipopolysaccharide (LPS)-binding protein and soluble CD14 function as accessory molecules for LPS-induced changes in endothelial barrier function, in vitro. *J. Clin. Invest.* 93:692-702, 1994.
7. Goldblum, S.E., X. Ding, T.W. Brann, and J. Campbell-Washington. Bacterial lipopolysaccharide induces actin reorganization, intercellular gap formation, and endothelial barrier dysfunction in pulmonary vascular endothelial cells: concurrent F-actin depolymerization and new actin synthesis. *J. Cell. Physiol.* 157:13-23, 1993.
8. Dejana, E., M. Corada, and M.G. Lampugnani. Endothelial cell-to-cell junctions. *FASEB J.* 9:910-

918, 1995.

9. Garcia, J.G., and K.L. Schaphorst. Regulation of endothelial cell gap formation and paracellular permeability. *J. Invest. Med.* 43:117-126, 1995.

10. Shasby, D.M., S.S. Shasby, J.M. Sullivan, and M.J. Peach. Role of endothelial cell cytoskeleton in control of endothelial permeability. *Circ. Res.* 51:657-661, 1982.

11. Volberg, T., Y Zick, R. Dror, I. Sabanay, C. Gilon, A. Levitzki, and B. Geiger. The effect of tyrosine-specific protein phosphorylation on the assembly of adherens-type junctions. *EMBO Journal.* 11:1733-1742, 1992.

12. Ulevitch, R.J., and P.S. Tobias. Recognition of endotoxin by cells leading to transmembrane signaling. *Curr. Opin. Immunol.* 6:125-130, 1994.

13. Arditi, M., J. Zhou, M. Torres, D.L. Durden, M. Stins, and K.S. Kim. Lipopolysaccharide stimulates the tyrosine phosphorylation of mitogen-activated protein kinases p44, p42, and p41 in vascular endothelial cells in a soluble CD14-dependent manner. *J. Immunol.* 155:3994-4003, 1995.

14. Novogrodsky, A., A. Vanichkin, M. Patya, A. Gazit, N. Osherov, and A. Levitzki. Prevention of Lipopolysaccharide-induced lethal toxicity by tyrosine kinase inhibitors. *Science.* 264:1319-1322, 1994

15. Alpert, G., G. Baldwin, C. Thompson, N. Wainwright, T.J. Novitsky, Z. Gillis, J. Parsonnet, G.R. Fleisher, and G.R. Siber. 1992. Limulus antilipopolysaccharide factor protects rabbits from meningococcal endotoxin shock. *J. Infect. Dis.* 165:494-500.

16. Cooperstock, M.S. 1974. Inactivation of endotoxin by polymyxin B. *Antimicrob. Agents Chemother.* 6:422-425

17. Morrison, D.C., and D.M. Jacobs. 1976. Binding of polymyxin B to the lipid A portion of bacterial lipopolysaccharides. *Immunochemistry.* 13:813-818.

18. Evans, T.J., A. Carpenter, D. Moyes, R. Martin, and J. Cohen. 1995. Protective effects of a recombinant amino-terminal fragment of human bactericidal/permeability-increasing protein in an animal model of gram negative sepsis. *J. Infect. Dis.* 171:153-160.

19. Hirata, M., J. Zhong, S.C. Wright, amd J.W. Larrick. 1995. Structure and functions of endotoxin-binding peptides derived from CAP18. *Prog. Clin. Biol. Res.* 392:317-326.

20. Levine, D.M., T.S. Parker, T.M. Donelly, A. Walsh, and A.L. Rubin. 1993. In vivo protection against endotoxin by plasma high density lipoprotein. *Proc. Natl.Acad. Sci.USA.* 90:12040- 12044.

21. Netea, M.G., P.N.M. Demacker, B.J. Kullberg, O.C. Boerman, I. Verschueren, A.F.H. Stalenhoef, and J.W.M. van der Meer. 1996. Low-density lipoprotein receptor-deficient mice are protected against lethal endotoxemia and severe Gram-negative infections. *J. Clin. Invest.* 97:1366-1372.

22. Morita, T., S. Ohtsubo, T. Nakamura, S. Tanaka, S. Iwanaga, K. Ohashi, and M. Niwa. 1985. Isolation and biological activities of limulus anticoagulant (anti-LPS factor) which interacts with lipopolysaccharide (LPS). *J. Biochem.* (Tokyo). 97:1611-1620.

23. Wainwright, N.R., R.J. Miller, E. Paus, T.J. Novitsky, M.A. Fletcher, T.M. McKenna, and T. Williams. 1990. Endotoxin binding and neutralizing activity by a protein from *Limulus polyphemus*. *In* Cellular and molecular aspects of endotoxin reactions. Elsevier Science Publishers. p. 315-325

24. Hoess, A., S. Watson, G.R. Siber, and R. Liddington. 1993. Crystal structure of endotoxin-neutralizing protein from the horseshoe crab, *Limulus* anti-LPS factor, at 1.5 A resolution. *EMBO J.* 12:3351-3356.

25. Muta T., T. Miyata, F. Tokunaga, T. Nakamura, and S. Iwanaga. 1987. Primary structure of anti-lipopolysaccharide factor from American horseshoe crab, *Limulus polyphemus*. *J. Biochem.* (Tokyo). 101:1321-1330.

26. Fletcher, M.A., T.M. Mckena, J.L Quance, N.R Wainwright, and T.J. Williams. 1993. Lipopolysaccharide detoxification by endotoxin neutralizing protein. *J. Surg. Res.* 55:147-154

27. Battafaraono, R.J., P.S. Dahlberg, C.A. Ratz, J.W. Johnston, B.H. Gray, J.R. Haseman, K.H. Mayo, and D.L. Dunn. 1995. Peptide derivatives of three distinct lipopolysaccharide binding proteins inhibit lipopolysaccharide-induced tumor necrosis factor-alpha secretion *in vitro*. *Surgery*. 118:318-324.

28. Warren, H.S., T.J. Novitsky, A. Bucklin, S.A. Kania, and G.R. Siber. 1987. Endotoxin neutralization with rabbit antisera to *Escherichia coli* J5 and other gram-negative bacteria. *Infect. Immun.* 55:1668-1673.

29. Choi, K. B., F. Wong, J. M. Harlan, P. M. Chaudhary, L. Hood, and A. Karsan. Lipopolysaccharide Mediates Endothelial Apoptosis by a FADD-dependent Pathway. *J Biol Chem* 273: 20185-8, 1998.

30. Frey, E. A., and B. B. Finlay. Lipopolysaccharide induces apoptosis in a bovine endothelial cell line via a soluble CD14 dependent pathway. *Microb Pathog* 24: 101-9, 1998.

31. Haimovitz-Friedman, A., C. Cordon-Cardo, S. Bayoumy, M. Garzotto, M. McLoughlin, R. Gallily, C. K. Edwards, 3rd, E. H. Schuchman, Z. Fuks, and R. Kolesnick. Lipopolysaccharide induces disseminated endothelial apoptosis requiring ceramide generation. *J Exp Med* 186: 1831-41, 1997.

32. Schumann, R. R., C. Belka, D. Reuter, N. Lamping, C. J. Kirschning, J. R. Weber, and D. Pfeil.

Lipopolysaccharide activates caspase-1 (interleukin-1-converting enzyme) in cultured monocytic and endothelial cells. *Blood* 91: 577-84, 1998

33. Brancolini, C., D. Lazarevic, J. Rodriguez, and C. Schneider. Dismantling cell-cell contacts during apoptosis is coupled to a caspase- dependent proteolytic cleavage of beta-catenin. *J Cell Biol* 139: 759-71, 1997.

34. Gervais, F. G., N. A. Thornberry, S. C. Ruffolo, D. W. Nicholson, and S. Roy. Caspases cleave focal adhesion kinase during apoptosis to generate a FRNK-like polypeptide [In Process Citation]. *J Biol Chem* 273: 17102-8, 1998.

35. Herren, B., B. Levkau, E. W. Raines, and R. Ross. Cleavage of beta-catenin and plakoglobin and shedding of VE-cadherin during endothelial apoptosis: evidence for a role for caspases and metalloproteinases. *Mol Biol Cell* 9: 1589-601, 1998.

36. Levkau, B., B. Herren, H. Koyama, R. Ross, and E. W. Raines. Caspase-mediated cleavage of focal adhesion kinase pp125FAK and disassembly of focal adhesions in human endothelial cell apoptosis. *J Exp Med* 187: 579-86, 1998.

37. Wen, L. P., J. A. Fahrni, S. Troie, J. L. Guan, K. Orth, and G. D. Rosen. Cleavage of focal adhesion kinase by caspases during apoptosis. *J Biol Chem* 272: 26056- 61, 1997.

38. Dubois, M., K. Giles, J. Hamilton, P. Rebers, and F. Smith. 1956. Colorimetric method for determination of sugars and related substances. *Anal. Chem.* 28:350-356.

39. Salomon, R. N., and S. Diaz-Cano. Introduction to apoptosis. *Diagn Mol Pathol* 4: 235-8, 1995.

(9) APPENDIX

A. Table 1 and 2

B. Figure Legends for Figure 1 – 26

C. Figures 1 - 26

A. Tables 1 and 2

TABLE 1 **ENP treatment either prior to or after LPS challenge does not protect against LPS-induced loss of endothelial monolayer barrier function.**

Pre-treatment	Treatment (5 min)	Post-treatment (6 h)	*n*	Mean ^{14}C-BSA Flux (pmol/h)[a] ± SE
——— [b]	———	———	70	0.010 ± 0.001
Medium	Medium	Medium	15	0.021 ± 0.001
Medium	LPS	Medium	25	0.087 ± 0.004[c]
ENP (0.5 h)	LPS	Medium	8	0.070 ± 0.005[c,d]
ENP (1.0 h)	LPS	Medium	8	0.078 ± 0.005[c,d]
Medium	LPS	ENP	14	0.082 ± 0.008[c,d]

[a] ^{14}C-albumin flux across LPS (10 ng/ml)- or media control-exposed monolayers that were either pre- or post-treated with ENP (1.0 ug/ml) or media alone.

[b] -, pretreatment baseline. The baseline barrier function for each monolayer was established prior to study; only monolayers which retained ≥ 97% of the ^{14}C-albumin tracer were studied.

[c] Significantly increased ($p < 0.001$) compared to media alone.

[d] Not significantly different ($p > 0.05$) compared to LPS alone.

Table 2 The Efficacy of Caspase or PTK Inhibition to Protect Against LPS-Induced EC Responses.

EC Responses to LPS	Caspase Inhibition (z-VAD-fmk)	PTK Inhibition (Herbimycin A)
Cleavage of ZA and FA Proteins	+	–
Endothelial Barrier Dysfunction	–	+
Endothelial Cell Detachment	+	+/-

B. Figure Legends for Figures 1 - 26

Figure 1: LPS-Induced Tyrosine Phosphorylation of EC Proteins. EC were incubated with: increasing concentrations of LPS for 1 h (A), LPS (100 ng/ml) (+) or media alone (-) for increasing exposure times (B), or increasing concentrations of the PTP inhibitor, sodium orthovanadate, in both the presence (+) and absence (-) of LPS (100 ng/ml) (C). EC lysates were resolved by SDS-PAGE, transferred to PVDF, probed with biotinylated anti-phosphotyrosine antibody, incubated with HRP-streptavidin, and developed with ECL. Approximate molecular weights in kDa are indicated by the arrows on the left. Each blot shown is representative of three separate experiments.

Figure 2. The Effects of PTK Inhibition on LPS-Induced Barrier Disruption and Protein Tyrosine Phosphorylation. Mean (± SE) transendothelial ^{14}C-BSA flux across monolayers (A) was assayed following exposure for 6 h to: media, LPS (100 ng/ml), herbimycin A (Herb A) (1 μM), genistein (Gen) (50 μg/ml), LPS and herbimycin A, and LPS and genistein. For all studies, herbimycin A and genistein were introduced at 16 h and 0.5 h prior to the LPS challenge, respectively. Transendothelial flux is expressed in pmol/h and *n* indicates the number of monolayers studied. The mean (± SE) baseline barrier function is indicated by the closed bars. * = significantly increased compared to simultaneous media controls. ** = significantly decreased compared to monolayers exposed to LPS alone. For Western blot analysis of protein tyrosine phosphorylation, EC monolayers were exposed for 1 h to the same conditions as those in the ^{14}C-BSA flux assay (B). EC lysates were resolved by SDS-PAGE, transferred to PVDF, and probed for phosphotyrosines. Arrow on the left indicates the approximate molecular weight of 66 kDa. This is a representative blot of three separate experiments.

Figure 3: The Effect of PTK Inhibition on LPS-Induced Intercellular Gap Formation. EC monolayers grown on filters were exposed for 6 h to media (A), herbimycin A (1 μM) (B), LPS (100

ng/ml) (C), or LPS in combination with herbimycin A (D). Herbimycin A was introduced 16 h prior to and throughout the 6 h LPS exposure. The monolayers were fixed, permeabilized, stained with fluorescein-phalloidin, and examined by epifluorescence microscopy. Arrows point to intercellular gaps. x 650.

Figure 4: The Effect of PTK Inhibition on LPS-Induced Increments of the G-Actin Pool and Decrements of the F-Actin Pool. For G- and F-actin measurements, monolayers were exposed for 6 h to media, LPS (100 ng/ml), herbimycin A (Herb A) (1 μM), genistein (Gen) (50 μg/ml), LPS with herbimycin A, or LPS with genistein. EC that were exposed to herbimycin A or genistein were pretreated for 16 h and 0.5 h, respectively. *n* for each control and experimental group is indicated within each bar. For the quantitation of the G-actin pool, EC were permeabilized and the G-actin-containing supernatants tested in the DNAse I inhibition assay standardized to pure G-actin (A). Each bar represents mean (±SE) G-actin in micrograms per milligram of total EC protein. * = significantly increased compared to the simultaneous media control. ** = significantly decreased compared to LPS alone. For the F-actin studies, monolayers were fixed, permeabilized, incubated with NBD-phallacidin, and extracted in methanol (B). The extracts were spectrofluorimetrically assayed and F-actin concentrations were expressed as mean (±SE) fluorescent units per milligram of total EC protein. * = significantly decreased compared to the simultaneous media control. ** = significantly increased compared to LPS alone.

Figure 5: The Effects of PTP Inhibition on LPS-Induced Increments of Transendothelial ^{14}C-BSA Flux. Mean (±SE) transendothelial ^{14}C-BSA flux across monolayers exposed for 6 h to media, LPS (10 ng/ml), vanadate (Van) (2.5 μM), PAO (0.1 μM), LPS with vanadate, or LPS with PAO is expressed in pmol/h. The mean (± SE) baseline barrier function is indicated by the closed bars. *n* indicates the number of monolayers studied. * = significantly increased compared to simultaneous media control. ** = significantly increased compared to LPS alone.

Figure 6: The Effects of PTP Inhibition on LPS-Induced Increments in the G-Actin Pool. EC were exposed for 6 h to media, LPS (10 ng/ml), vanadate (Van) (2.5 μM), PAO (0.1 μM), LPS with vanadate, or LPS with PAO. For G-actin measurements, EC were permeabilized and the G-actin-containing supernatants tested in the DNAse 1 inhibition assay standardized to pure G-actin. Each bar represents the mean (±SE) G-actin in micrograms per milligram of total EC protein. *n* indicates the number of monolayers studied. * = significantly increased compared to simultaneous media control. ** = significantly increased compared to LPS alone.

Figure 7: Immunolocalization of Phosphotyrosine-Containing Proteins. EC monolayers grown on filters were exposed for 1 h to media (A) or LPS (100 ng/ml) (B). Monolayers were subsequently fixed, permeabilized, stained with FITC-conjugated anti-phosphotyrosine antibody, and visualized through an epifluorescence microscope. In LPS-exposed EC (B), arrows indicate phosphotyrosine-containing proteins forming plaque-like structures compatible with FAs. In the same cells (B), arrow heads indicate phosphotyrosine-containing proteins forming a semi-continuous band around the cell periphery. x 1000.

Figure 8: Identification of Paxillin as the Substrate for Increased Tyrosine Phosphorylation in EC Exposed to LPS. EC were exposed to LPS (100 ng/ml, 1 h) and lysed with modified RIPA buffer. The EC lysates were incubated with either anti-phosphotyrosine (PY20) or anti-paxillin murine antibodies, followed by incubation with anti-mouse IgG cross-linked to agarose. The resulting immunoprecipitates were resolved by SDS-PAGE and transferred onto PVDF. The blots were probed with biotinylated anti-phosphotyrosine antibodies (4G10) followed by HRP-conjugated streptavidin, or anti-paxillin antibodies followed by incubation with HRP-conjugated anti-murine IgG antibody. All blots were developed with enhanced chemiluminescence (A). IP = immunoprecipitate. IB = immunoblot. The additional bands seen in the two lanes immunoblotted for paxillin represent the heavy chains of the immunoprecipitating antibody under denaturing conditions. In other experiments, media and LPS-exposed EC whole cell

lysates were resolved by SDS-PAGE in parallel with LPS-exposed EC lysates immunodepleted with anti-paxillin antibody (ID). The immunoprecipitate, containing the paxillin that was immunodepleted from the LPS-exposed EC lysate, was also studied (IP). The lysates were subsequently transferred to PVDF, and probed with the biotinylated anti-phosphotyrosine antibody followed by HRP-conjugated steptavidin (B).

Figure 9. Colocalization of Paxillin and Phosphotyrosine-containing Proteins. EC monolayers grown on filters were exposed for 1 h to either media (A-C) or LPS (100 ng/ml) (D-F). The monolayers were then fixed, permeabilized, incubated with murine anti-paxillin antibody, washed, and subsequently incubated with Texas Red-conjugated anti-mouse IgG. After vigorous washing, the monolayers were then stained with FITC-conjugated anti-phosphotyrosine antibody, and visualized through an epifluorescence microscope. Green signal indicates phosphotyrosine-containing proteins (A,D), red signal indicates paxillin (B,E), and yellow signal indicates colocalization of the two probes (C,F). Arrows indicate selected discrete areas that display both phosphotyrosine (D) and paxillin (E) signals, as well as, their colocalization (F). (x 550).

Figure 10: Effects of LPS fractions on transendothelial ^{14}C-BSA flux. A. Transendothelial ^{14}C-BSA flux across monolayers was assayed after exposure for 6 h to increasing concentrations of either the lipid A fraction (cross-hatched bars) or the O-specific polysaccharide fraction (open bars) derived from *E. coli* 0111:B4 LPS. Each bar represents mean ($\pm$ SE) transendothelial ^{14}C-BSA flux in pmol/h. Pretreatment baseline ^{14}C-BSA flux across monolayers exposed to either lipid A or O-specific polysaccharide fractions as well as ^{14}C-BSA flux across naked filters (closed bar) are also shown. * Significantly increased compared with simultaneous media control. *n*, number of monolayers studied. **B.** EC monolayers were assayed for transendothelial ^{14}C-BSA flux immediately after 6 h exposures to media alone (open bar), PMB (10,000 ng/ml) (gray bar), LPS (10 ng/ml) (cross-

hatched bar), or LPS (10 ng/ml) coadministered with increasing concentrations of PMB (vertical striped bars). Mean (± SE) pretreatment baseline ^{14}C-BSA flux is represented by the closed bar. * Significantly increased compared to media control. ** Significantly decreased compared to LPS. *n*, number of monolayers studied.

Figure 11: Dose-dependent effects of ENP on LPS-induced barrier dysfunction. Baseline barrier function (closed bar) was determined for all monolayers prior to treatment. Transendothelial ^{14}C-BSA flux across monolayers was assayed after exposure for 6 h to media (open bar), ENP (10^4 ng/ml) (gray bar), LPS (10 ng/ml) (cross-hatched bar), or LPS coadministered with increasing concentrations of ENP (vertical striped bars). Each bar represents mean (± SE) transendothelial ^{14}C-BSA flux in pmol/h. * Significantly increased compared to media control. ** Significantly decreased compared to LPS alone. *n*, number of monolayers studied. *** Significantly decreased compared to LPS alone, but not significantly different from media alone.

Figure 12: Effect of ENP on LPS-induced tyrosine phosphorylation of a 66 kDa EC protein. For Western blot analysis of protein tyrosine phosphorylation, EC monolayers were exposed to media, ENP (1.0 μg/ml), LPS (100 ng/ml), or LPS coadministered with ENP for 1 h. The EC lysates were resolved by SDS-PAGE, transferred to polyvinylidine difluoride membrane, and probed for phosphotyrosines. Molecular weights (kDa) are indicated by arrows on left. Blot is representative of 3 separate experiments.

Figure 13: Effect of ENP on phosphotyrosine-containing proteins in LPS-exposed EC. EC monolayers grown on filters were exposed for 1 h to media (A), ENP (1.0 μg/ml) (B), LPS (100 ng/ml) (C), or LPS coadministered with ENP (D). The monolayers were fixed, probed with FITC-conjugated anti-phosphotyrosine antibody, and photographed through an epifluorescence microscope. Arrows indicate phosphotyrosine signal at intercellular boundaries. Magnification, x600.

Figure 14: Effects of ENP on LPS-induced changes in the F- and G-actin pools. For G- and F-actin measurements, monolayers were exposed for 6 h to media (open bar), ENP (100 ng/ml) (gray bar), LPS (10 ng/ml) (cross-hatched bar), or LPS coadministered with ENP (vertical striped bar). **A.** For the F-actin studies, monolayers were fixed, permeabilized, incubated with NBD-phallicidin, and extracted with methanol. The extracts were spectrofluorimetrically assayed and F-actin concentrations expressed as mean (± SE) fluorescent units per mg of total EC protein. * Significantly decreased compared to media control. ** Significantly increased compared to LPS alone, but not significantly decreased compared to media alone. **B.** For the quantitation of the G-actin pool, EC were permeabilized and the G-actin containing supernatants tested in the DNAse I inhibition assay standardized to pure G-actin. Each bar represents mean (± SE) G-actin expressed in μg/mg total EC protein. * Significantly increased compared to media control. ** Significantly decreased compared to LPS alone, but not significantly increased compared to media alone. *n* for each experimental group is indicated in each bar.

Figure 15: ENP crossprotects against a wide variety of endotoxins. Transendothelial ^{14}C-BSA flux was assayed immediately following 6 h exposures to media (open bar), equivalent concentrations based on KDO content of LPS derived from *E. coli* O111:B4 (10 ng/ml), *E. coli* 055:B5, *P. aeruginosa*, *K. pneumoniae*, *S. marcescens,* or *S. minnesota* (crosshatched bars), or these same LPS preparations coadministered with ENP (100 ng/ml) (gray bars). Each bar represents mean (± SE) transendothelial ^{14}C-BSA flux in pmol/h. Baseline barrier function (closed bar) for all monolayers studied is indicated. * Significantly decreased compared to LPS alone at $p < 0.05$, but not significantly increased compared to media control.

Figure 16: Dose- and Time-Dependent Effect of LPS on Transendothelial ^{14}C-BSA Flux and EC Detachment. Vertical bars represent mean (±SE) transendothelial ^{14}C-BSA flux in pmol/h (A, B) or

percent EC detachment from gelatin-impregnated filters (C, D) immediately after a 6 h exposure to increasing concentrations of LPS (A, C), or after increasing exposure times to a fixed concentration of LPS (10 ng/ml) or medium alone (B, D). *n* for each experimental condition is notated within each bar. * = significantly increased compared to the simultaneous medium control.

exposure times (B). EC DNA was isolated and subjected to gel electrophoresis in a 2% agarose gel stained with ethidium bromide. Bands were visualized with UV light. DNA molecular weight markers, expressed as base pairs (bp), are indicated to the left of each gel. Each gel is representative of three separate experiments.

Figure 17: LPS-Induced EC DNA Fragmentation. EC were incubated with either increasing concentrations of LPS for 6 h (A), or a fixed concentration of LPS (100 ng/ml) (+) or medium alone (-) for increasing exposure times (B). EC DNA was isolated and subjected to gel electrophoresis in a 2% agarose gel stained with ethidium bromide. Bands were visualized with UV light. DNA molecular weight markers, expressed as base pairs (bp), are indicated to the left of each gel. Each gel is representative of three separate experiments.

Figure 18: Dose- and Time-Dependent Effect of LPS On Cleavage of ZA Component Proteins. EC were incubated with either increasing concentrations of LPS for 6 h (A), or a fixed concentration of LPS (100 ng/ml) (+) or medium alone (-) for increasing exposure times (B). EC lysates were immunoblotted with antibodies raised against cadherin, $p120^{Cas}$, α-catenin, β-catenin, or γ-catenin. Molecular mass (in thousands) is indicated by arrows to the right. Each blot is representative of three separate experiments.

Figure 19: Dose- and Time-Dependent Effect of LPS On Cleavage of FA Component Proteins. EC were incubated with either increasing concentrations of LPS for 6 h (A), or a fixed concentration of LPS (100 ng/ml) (+) or medium alone (-) for increasing exposure times (B). EC lysates were immunoblotted with anti-$p130^{Cas}$ or anti-FAK antibodies and then stripped and reprobed for β-tubulin. Molecular mass

(in thousands) is indicated by arrows to the right. Each blot is representative of three separate experiments.

Figure 20: Caspase Inhibition Protects Against LPS-Induced Protein Cleavage and Apoptosis. EC were incubated for 4 h with medium, caspase inhibitor (z-VAD; 100 μM, LPS (100 ng/ml), LPS in the presence of increasing concentrations of z-VAD, or LPS in the presence of z-FA-fmk (100 μM), a negative control (NC) peptide (A). The caspase inhibitor or NC peptide was introduced 2 h prior to and throughout the 4 h LPS exposure. EC lysates were immunoblotted with antibodies raised against β-catenin, γ-catenin, or FAK. Each blot is representative of three separate experiments. Apoptosis was detected by DNA laddering (B) and TUNEL staining (C). EC were incubated for 4 h with medium, caspase inhibitor (z-VAD; 100 μM), LPS (100 ng/ml), or LPS with z-VAD. EC DNA was electrophoresed through a 2% agarose gel stained with ethidium bromide (B). Bands were visualized with ultraviolet light. DNA molecular weight markers, expressed as base pairs (bp), are indicated to the left. In other experiments, EC monolayers were fixed, permeabilized, and assessed for apoptosis by the TUNEL assay (C) (i, medium control; ii, z-VAD; iii, LPS with z-VAD; and iv-vi, LPS alone). Arrows and arrowheads indicate apoptotic bodies and condensed nuclear chromatin, respectively. Magnification, x 450.

Figure 21: Effect of Caspase Inhibition on LPS-Induced Increments in Transendothelial Albumin Flux. Vertical bars represent mean (±SE) transendothelial ^{14}C-BSA flux in pmol/h immediately after a 4 h exposure to medium, z-VAD (100 μM), herbimycin A (Herb A; 1 μM) LPS (100 ng/ml), LPS + z-VAD, and LPS + Herb A. For all studies, z-VAD and Herb A were introduced 2 and 16 h, respectively, prior to and throughout the LPS challenge. *, significantly increased compared to media alone; **, significantly decreased compared to LPS alone but not significantly increased compared to media alone. *n* for each experimental group is indicated in each bar. In other experiments, EC seeded on cell culture

dishes were treated identically as above, and immunoblotted with anti-β-catenin antibodies (insert). Each lane number in brackets corresponds with the same number and treatment under each vertical bar. The blot is representative of three separate experiments.

Figure 22: Effect of LPS-Induced β-Catenin Cleavage on β-Catenin-Protein Interactions. Lysates of EC exposed for 6 h to LPS (100 ng/ml; +) or medium alone (-) were immunoblotted with anti-β-catenin antibodies raised against either the COOH- or NH_2-terminus (A). In other experiments, lysates of EC similarly exposed to LPS or medium alone were incubated with anti-cadherin, anti-α-catenin, or anti-APC antibodies followed by anti-mouse or anti-rabbit IgG cross-linked to agarose (B). The immunoprecipitated proteins were resolved by SDS-PAGE, transferred to PVDF, and immunoblotted with an antibody raised against the COOH-terminus of β-catenin. The left panel represents whole cell lysates probed with anti-β-catenin antibody. Each blot is representative of three separate experiments.

Figure 23: Caspase Inhibition Protects Against LPS-Induced EC Detachment. (A) Vertical bars represent mean (±SE) percent EC detachment from gelatin-impregnated filters immediately after a 4 h exposure to medium, z-VAD (100 μM), herbimycin A (Herb A; 1 μM, LPS (100 ng/ml), LPS + z-VAD, or LPS + Herb A. For all studies, z-VAD and Herb A were introduced 2 and 16 h, respectively, prior to and throughout the LPS challenge. *, significantly increased compared to medium alone; **, significantly decreased compared to LPS alone but not significantly increased compared to medium alone; ***, significantly decreased compared to LPS alone and significantly increased compared to medium alone. *n* for each experimental group is indicated in each bar. (B) In other studies, EC cultured in plastic dishes were incubated for 4 h with i) medium, ii) z-VAD (100 μM), iii) Herb A (1 μM), iv) a control peptide, z-FA-fmk (100 μM) LPS alone (100 ng/ml), vi) LPS + z-VAD, vii) LPS + Herb A, or viii) LPS + z-FA-fmk, and then visualized by phase contrast microscopy. Magnification, x 35.

Figure 24: Effect of FAK Cleavage on Its Association With and Tyrosine Phosphorylation of

Paxillin. Lysates of EC exposed for 6 h to LPS (100 ng/ml; +) or medium alone (-) were immunoprecipitated with anti-paxillin antibodies and immunoblotted with a murine monoclonal antibody raised against FAK (A). The left two lanes represent whole cell lysates probed with anti-FAK antibody. In other experiments, paxillin was immunoprecipitated from lysates of EC after increasing exposure times to LPS (100 ng/ml; +) or media alone (-) (B), or to EC treated for 6 h with LPS (100 ng/ml) or medium, in the presence or absence of z-VAD (100 μM) (C). Blots of these paxillin immunoprecipitates were probed with biotinylated anti-phosphotyrosine antibody (4G10). All blots (A,B,C) were stripped and reprobed for paxillin (*IB). Laser densitometry to quantitate panels B and C is shown (D). Each blot is representative of three separate experiments.

Figure 25: LPS-Induced EC Protein Cleavage is Blocked by Lipid A Neutralizing Proteins and Mimicked by EC Exposure to Either SEB or TNFα. EC were incubated for 4 h with medium, ENP (1 μg/ml), PMB (10 μg/ml), LPS (100 ng/ml), or LPS in the presence of ENP or PMB (A). In other experiments, EC were incubated for 4 h with either media, LPS (100 ng/ml), SEB (100 μg/ml), or TNFα (500 U/ml) (B). EC lysates were immunoblotted with either anti-β-catenin or anti-FAK antibodies. Each blot is representative of three separate experiments.

Figure 26: Hypothetical Schema for LPS-Induced Disruption of Endothelial Monolayer Integrity. LPS-induced loss of endothelial barrier function and EC detachment may be mechanistically linked to the activation of protein tyrosine kinases (PTKs) and/or caspases. LPS induces the activation of EC PTKs and a transient state of increased protein tyrosine phosphorylation. PTK inhibition protects against LPS-induced intercellular gap formation, actin depolymerization, and loss of barrier function. LPS also activates caspases which cleave the zonula adherens proteins, β- and γ-catenin, as well as, the focal adhesion proteins, focal adhesion kinase (FAK) and $p130^{Cas}$. The cleavage of β- and γ-catenin does not appear to alter their binding to α-catenin. Cleavage of FAK leads to the dissociation of its kinase domain

from another focal adhesion constituent protein and FAK substrate, paxillin, resulting in decreased tyrosine phosphorylation of the latter. This may, in turn, disrupt the ability of focal adhesions to participate in cell adherence to the underlying extracellular matrix and/or disrupt integrin-mediated, cell-survival signaling.

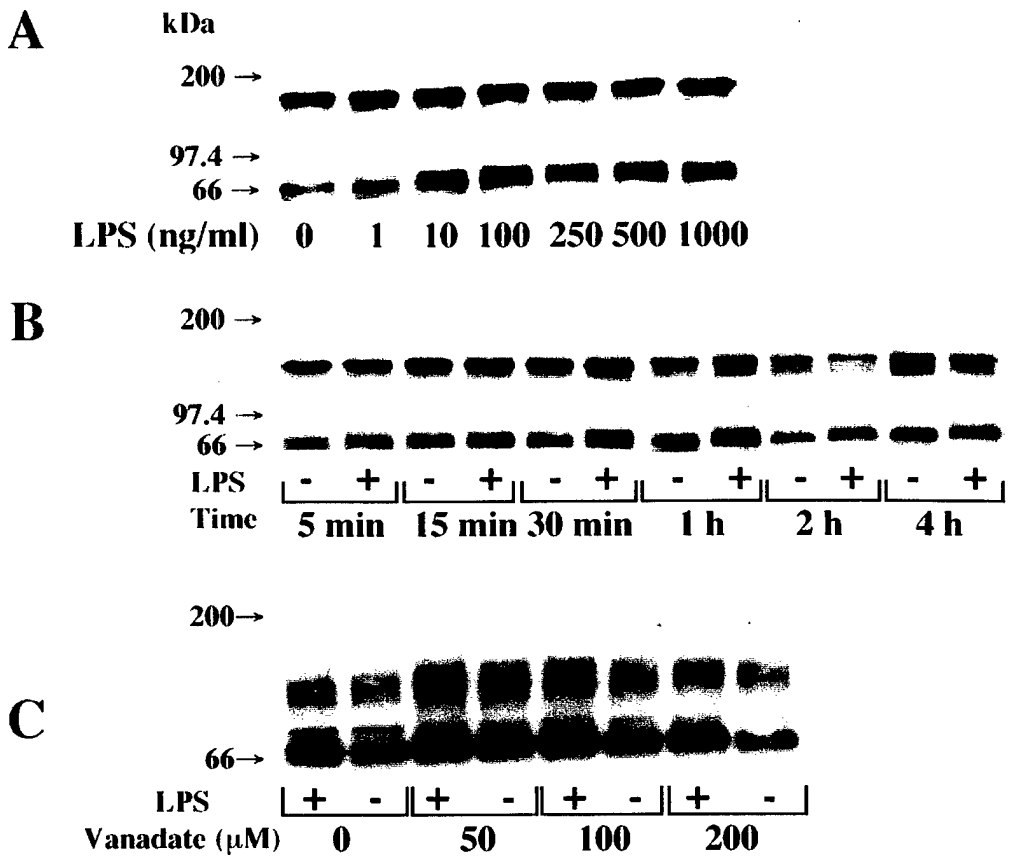
A
kDa
200 →
97.4 →
66 →
LPS (ng/ml) 0 1 10 100 250 500 1000
B
200 →
97.4 →
66 →
LPS - + - + - + - + - + - +
Time 5 min 15 min 30 min 1 h 2 h 4 h
C
200→
66→
LPS + - + - + - + -
Vanadate (μM) 0 50 100 200

Fig 1

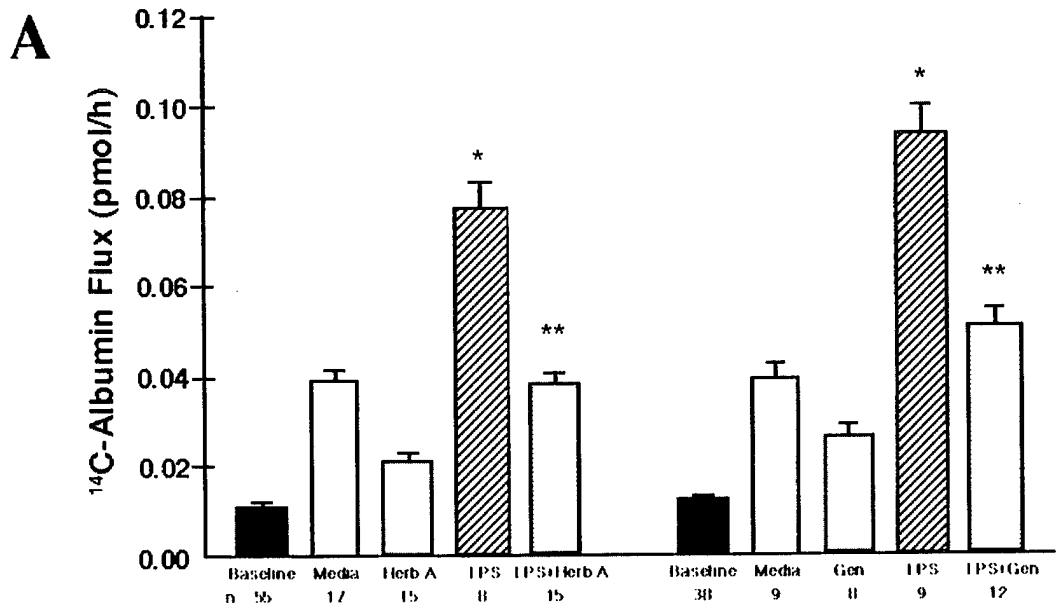
A
0.12
0.10
0.08
0.06
0.04
0.02
0.00
^{14}C-Albumin Flux (pmol/h)
*
**
*
**
Baseline
Media
Herb A
LPS
LPS+Herb A
Baseline
Media
Gen
LPS
LPS+Gen
n 56
17
15
8
15
38
9
8
9
12

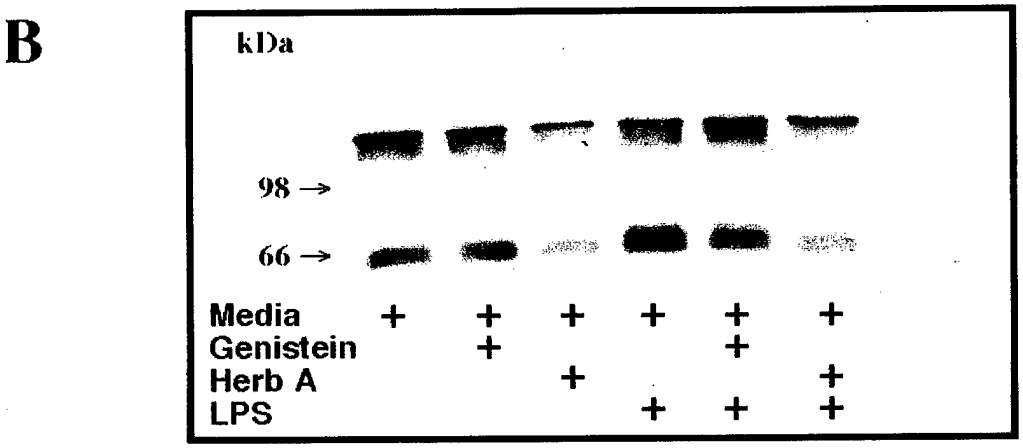
B
kDa
98 →
66 →
Media + + + + + +
Genistein + +
Herb A + +
LPS + + +

Fig 2

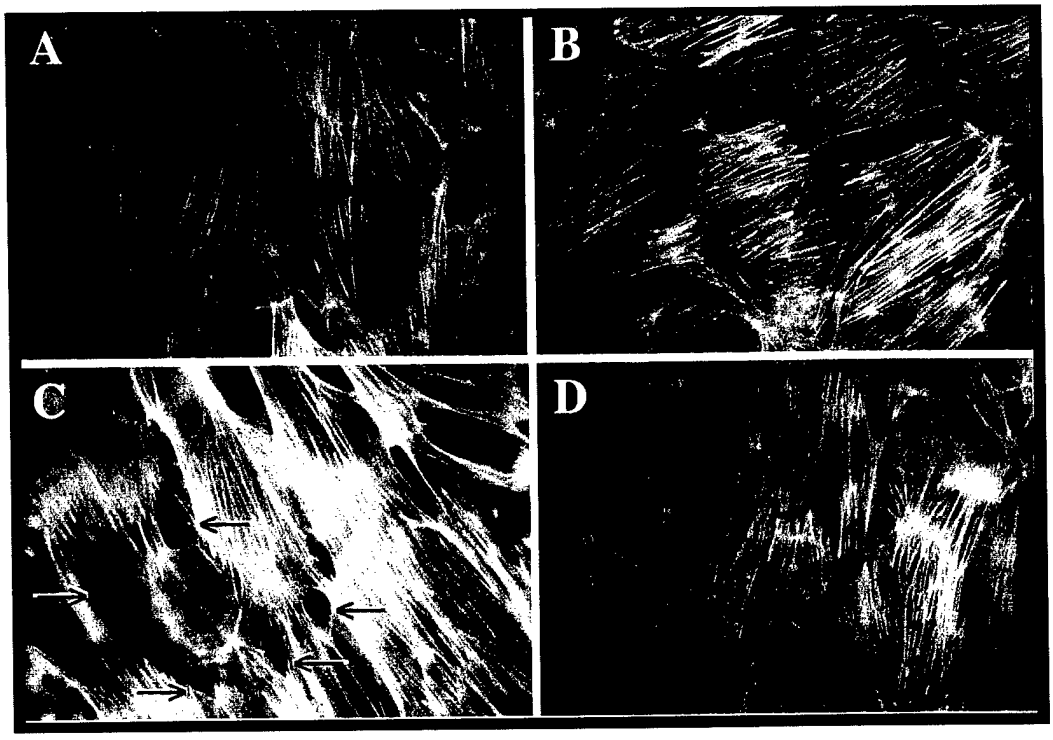

Fig 3

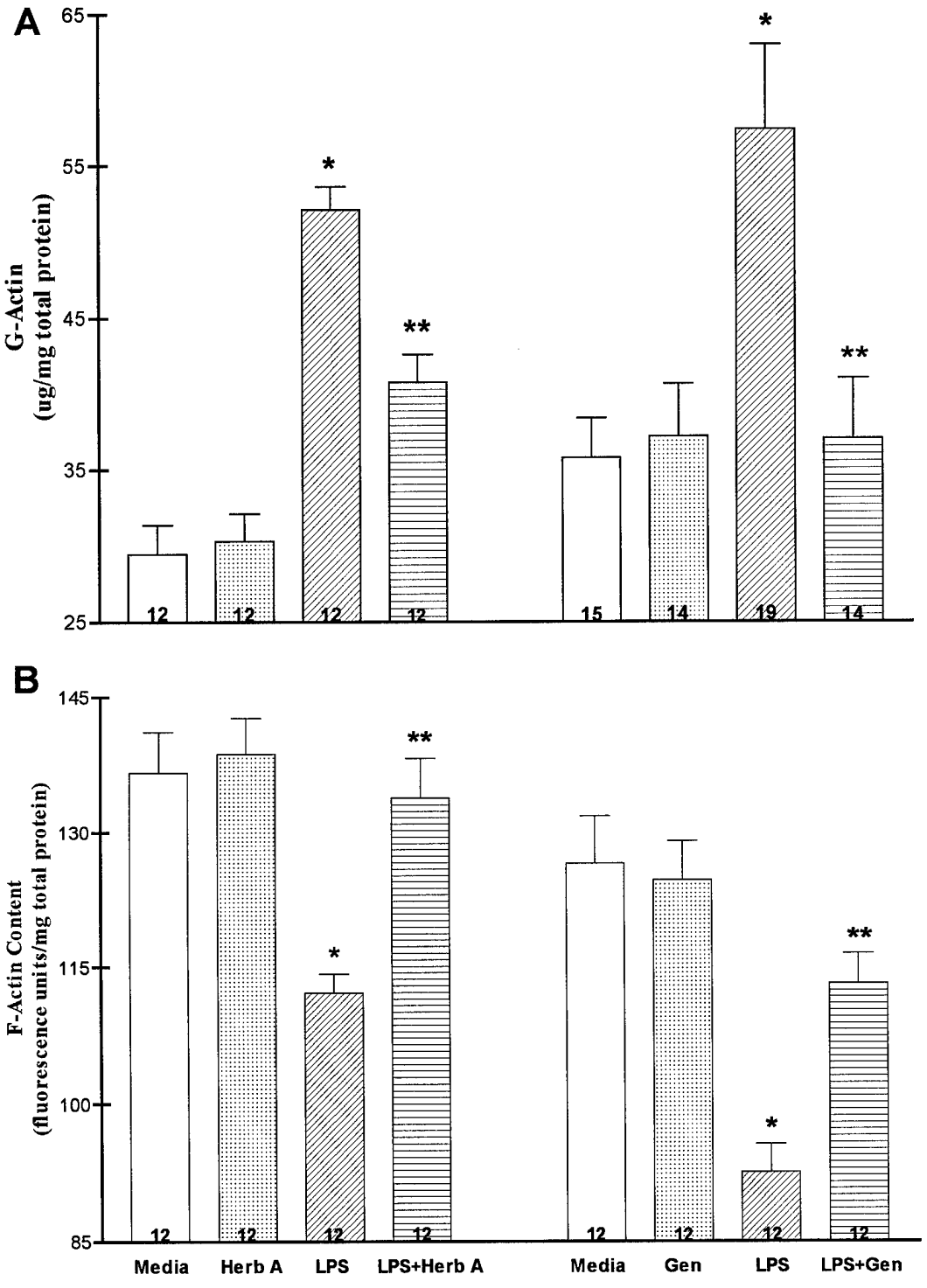
A
G-Actin
(ug/mg total protein)
65
55
45
35
25
12
12
12
12
15
14
19
14
*
**
*
**
B
F-Actin Content
(fluorescence units/mg total protein)
145
130
115
100
85
12
12
12
12
12
12
12
12
*
**
*
**
Media
Herb A
LPS
LPS+Herb A
Media
Gen
LPS
LPS+Gen

Fig 4

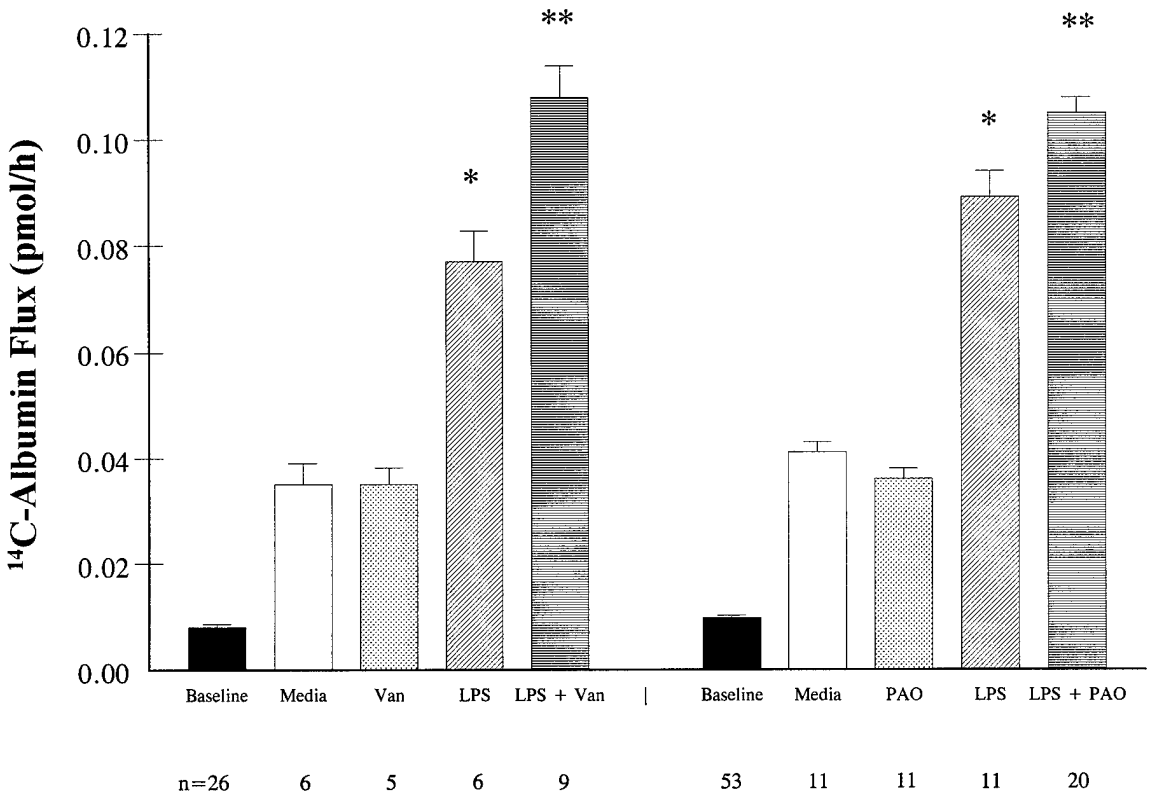
^{14}C-Albumin Flux (pmol/h)
0.12
0.10
0.08
0.06
0.04
0.02
0.00
*
**
*
**
Baseline
Media
Van
LPS
LPS + Van
Baseline
Media
PAO
LPS
LPS + PAO
n=26
6
5
6
9
53
11
11
11
20

Fig 5

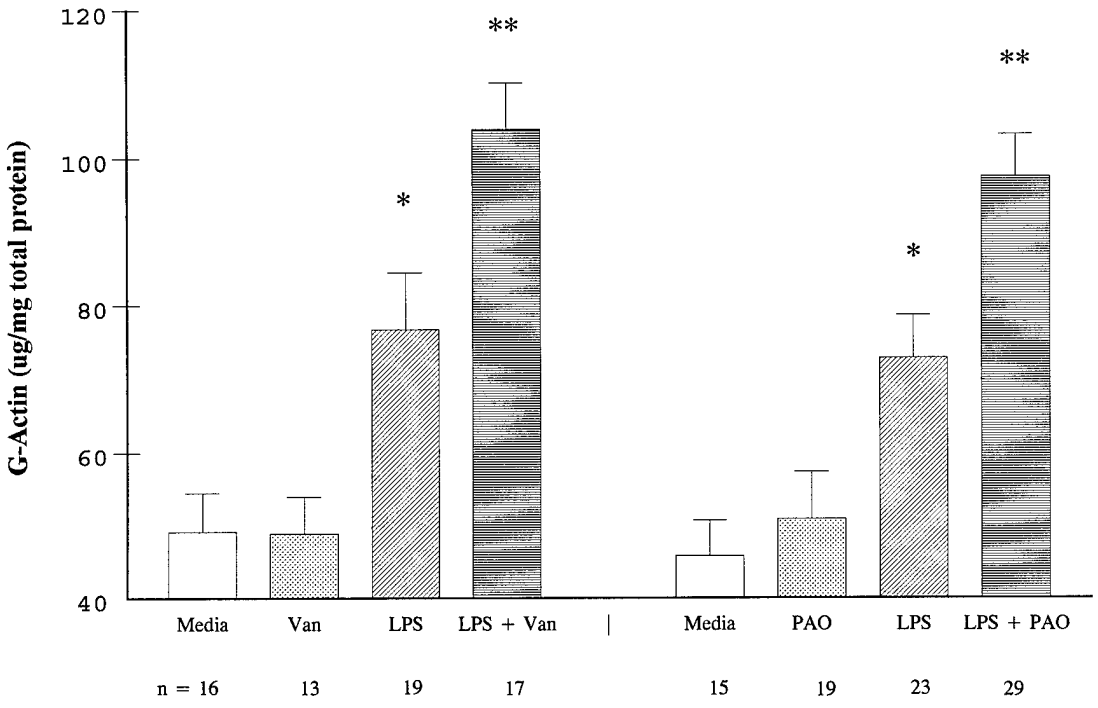
G-Actin (ug/mg total protein)
120
100
80
60
40
**
*
**
*
Media
Van
LPS
LPS + Van
Media
PAO
LPS
LPS + PAO
n = 16
13
19
17
15
19
23
29

Fig 6

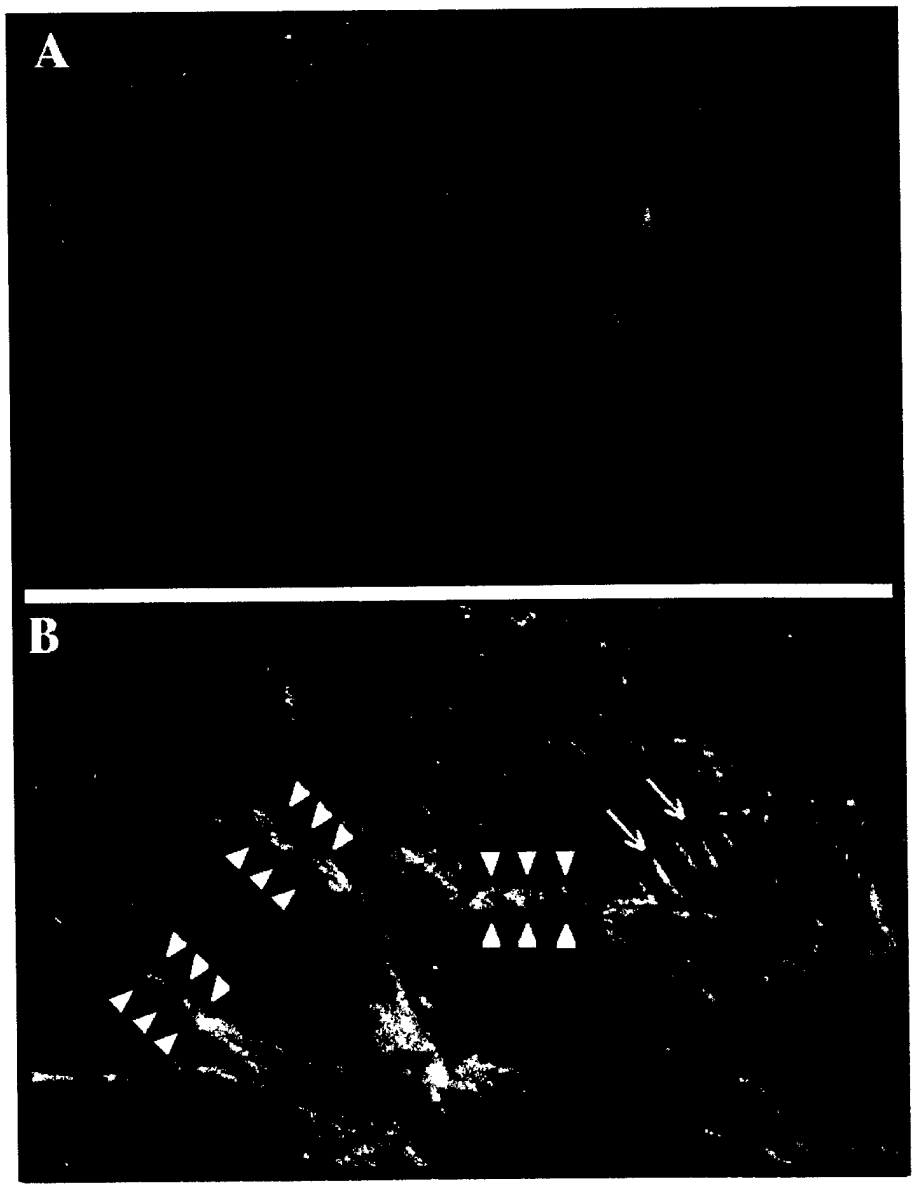

Fig 7

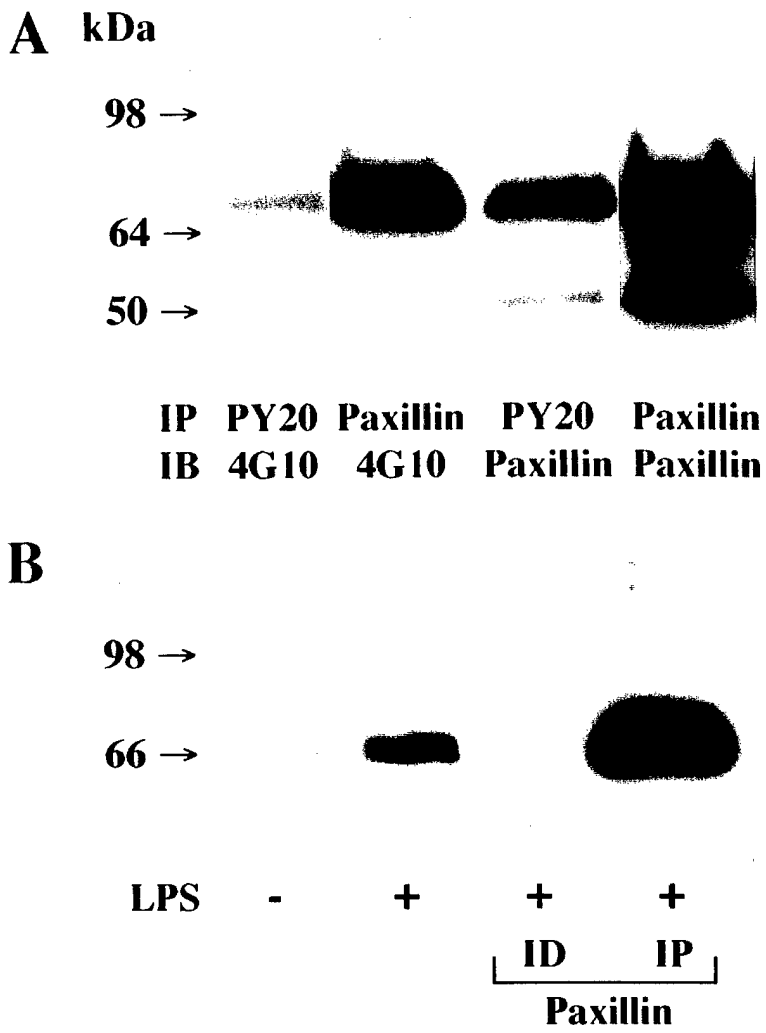
A
kDa
98 →
64 →
50 →
IP PY20 Paxillin PY20 Paxillin
IB 4G10 4G10 Paxillin Paxillin
B
98 →
66 →
LPS - + + +
ID IP
Paxillin

Fig 8

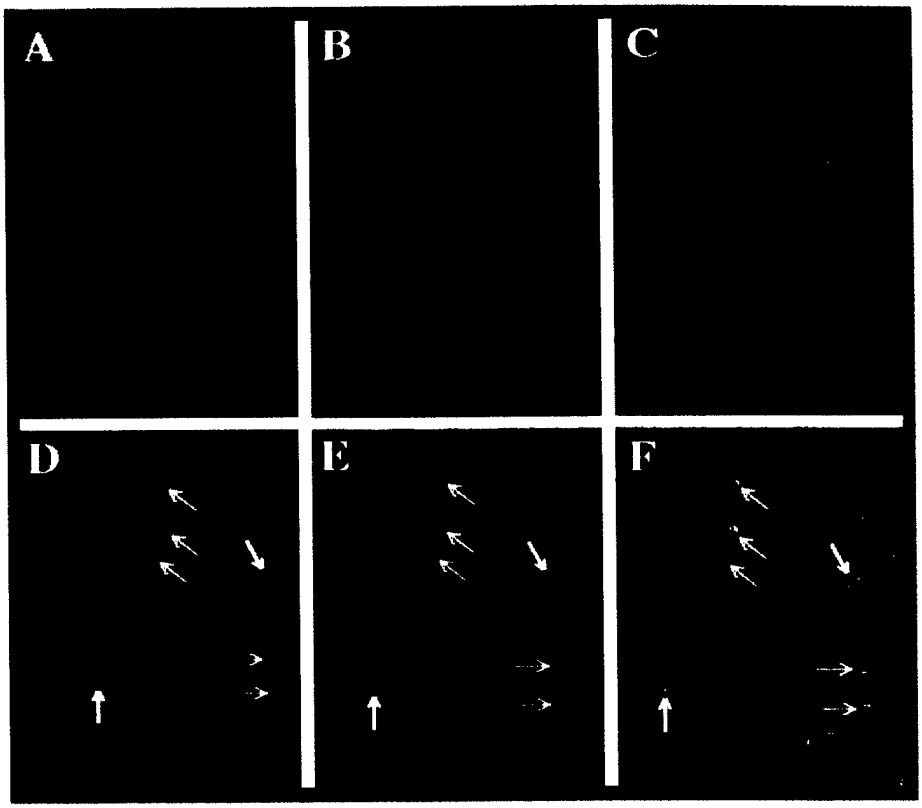

Fig 9

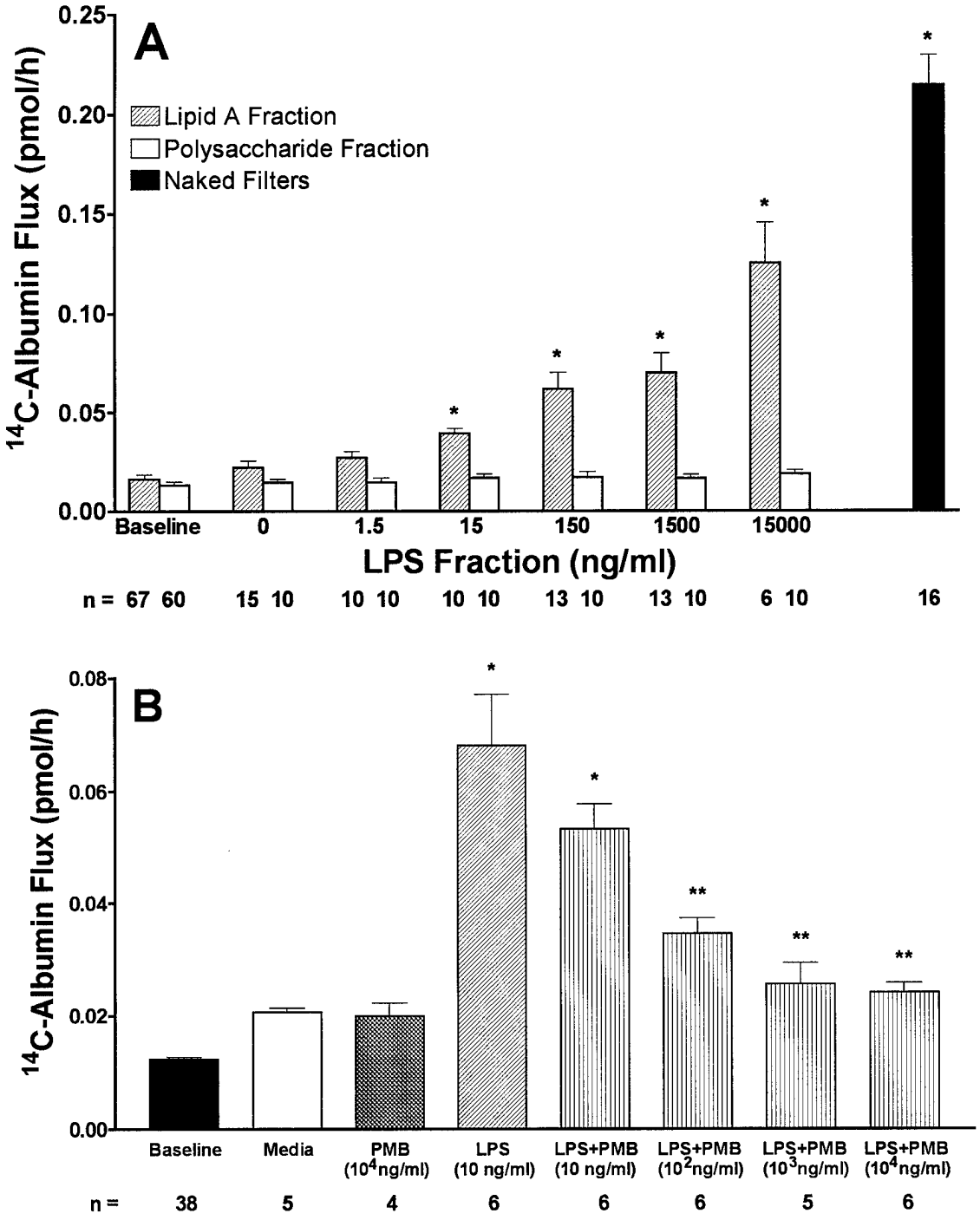
A
Lipid A Fraction
Polysaccharide Fraction
Naked Filters
^{14}C-Albumin Flux (pmol/h)
0.25
0.20
0.15
0.10
0.05
0.00
Baseline
0
1.5
15
150
1500
15000
LPS Fraction (ng/ml)
n = 67 60 15 10 10 10 10 10 13 10 13 10 6 10 16
B
^{14}C-Albumin Flux (pmol/h)
0.08
0.06
0.04
0.02
0.00
Baseline
Media
PMB (10^4ng/ml)
LPS (10 ng/ml)
LPS+PMB (10 ng/ml)
LPS+PMB (10^2ng/ml)
LPS+PMB (10^3ng/ml)
LPS+PMB (10^4ng/ml)
n = 38 5 4 6 6 6 5 6

Fig 10

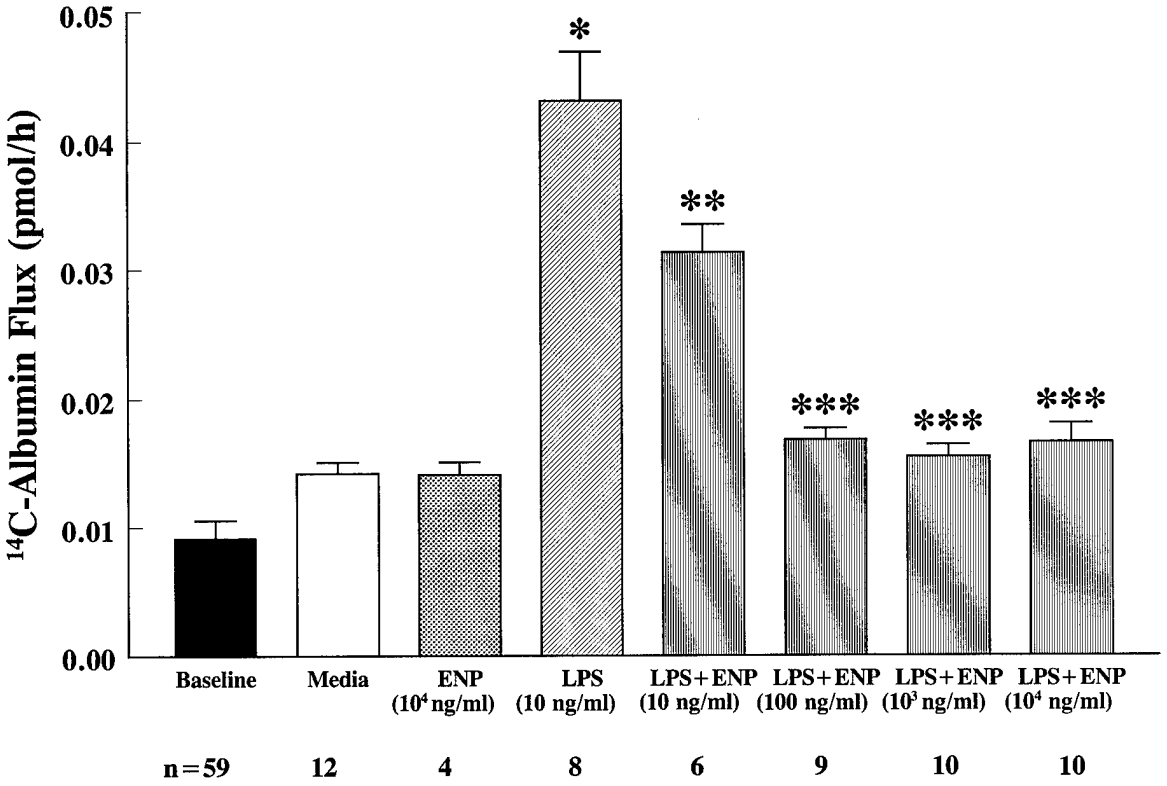
0.05
0.04
0.03
0.02
0.01
0.00
^{14}C-Albumin Flux (pmol/h)
*
**
***
***
***
Baseline
Media
ENP (10^4 ng/ml)
LPS (10 ng/ml)
LPS+ENP (10 ng/ml)
LPS+ENP (100 ng/ml)
LPS+ENP (10^3 ng/ml)
LPS+ENP (10^4 ng/ml)
n=59
12
4
8
6
9
10
10

Fig 11

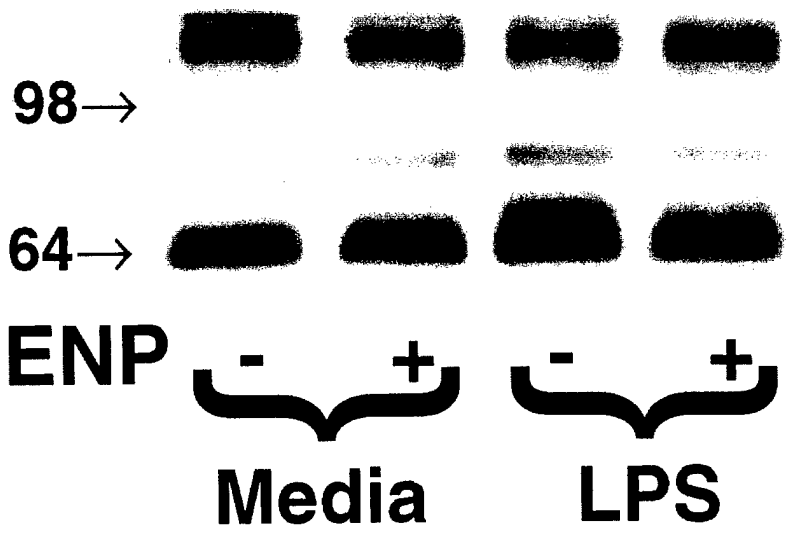

Fig 12

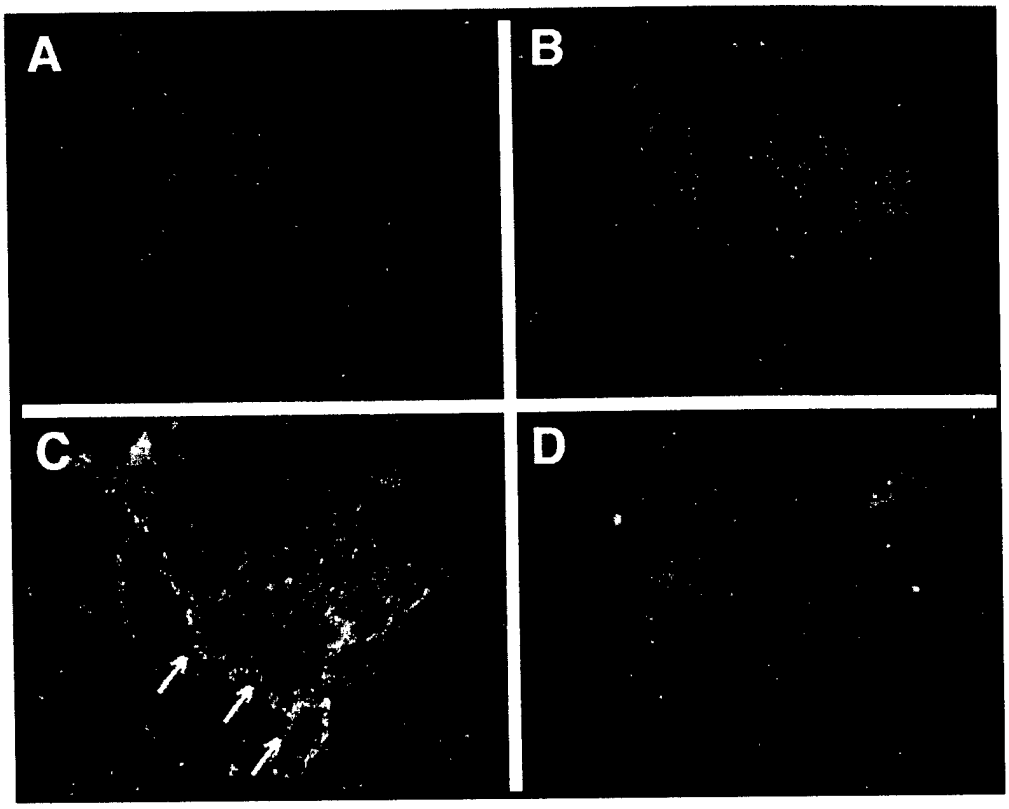

Fig 13

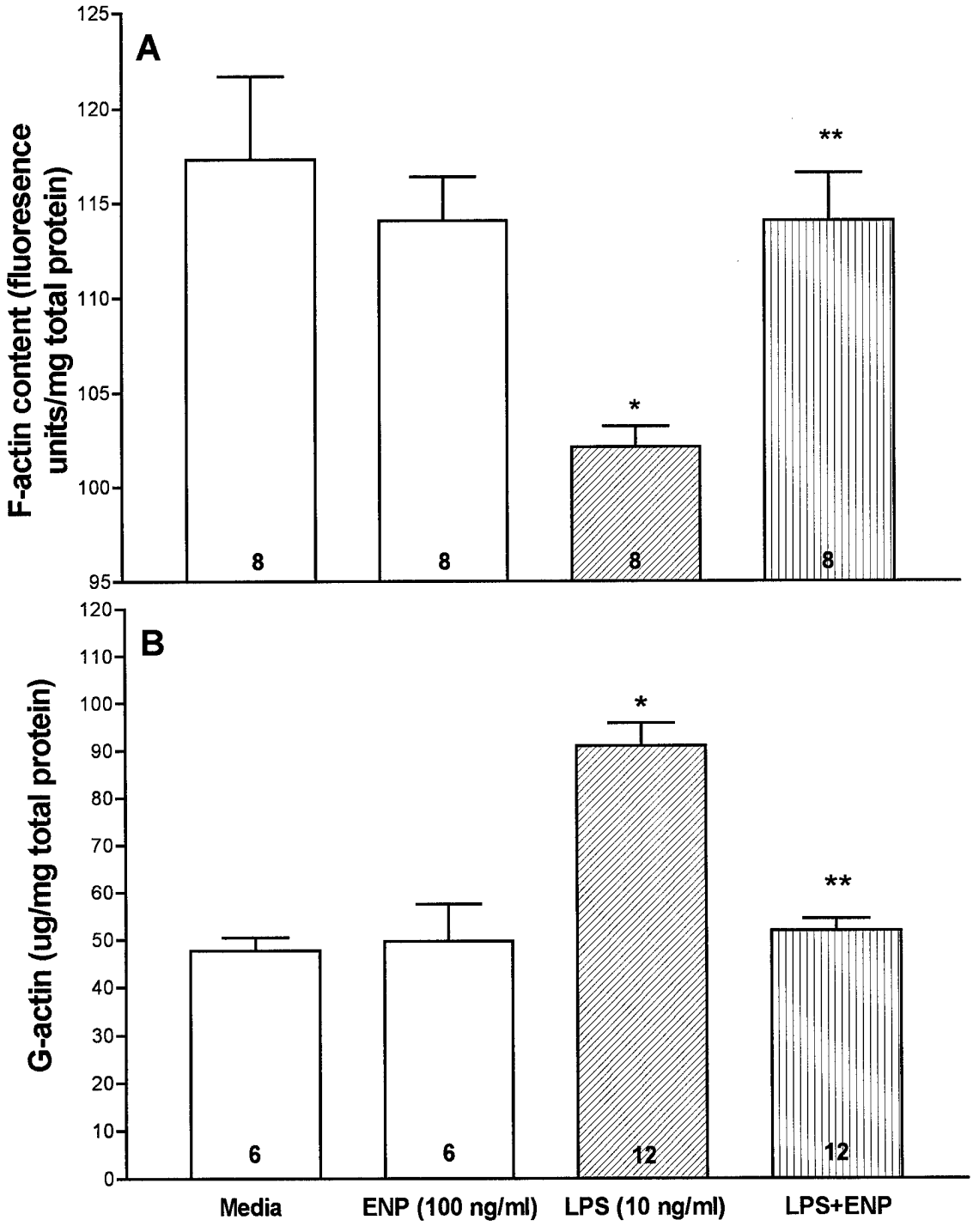
A
F-actin content (fluoresence units/mg total protein)
125
120
115
110
105
100
95
8
8
*
8
**
8
B
G-actin (ug/mg total protein)
120
110
100
90
80
70
60
50
40
30
20
10
0
6
6
*
12
**
12
Media
ENP (100 ng/ml)
LPS (10 ng/ml)
LPS+ENP

Fig 14

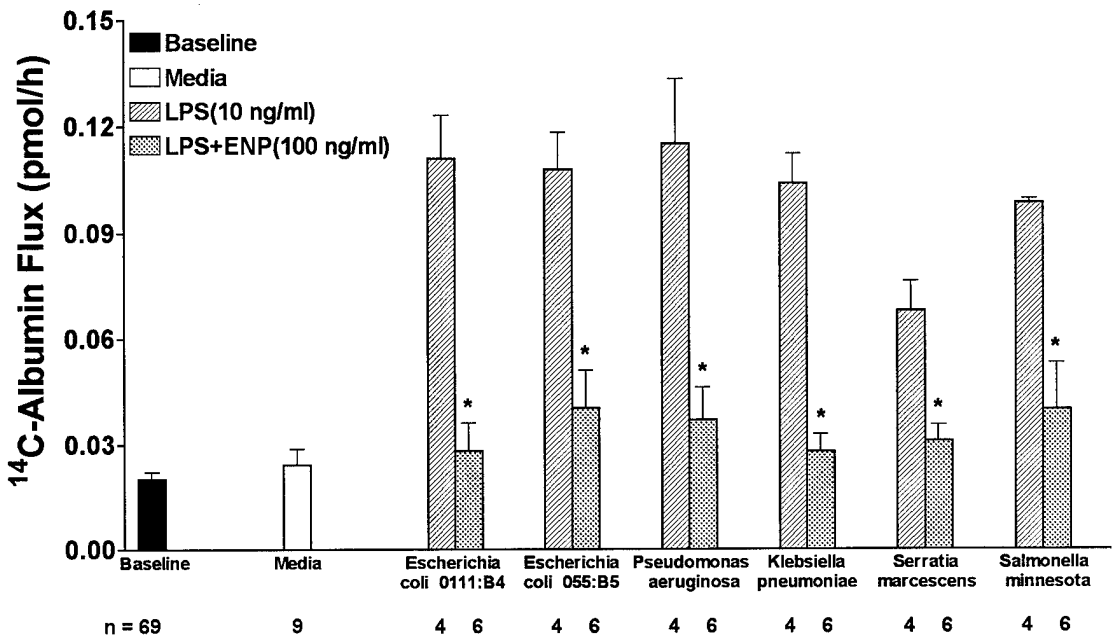
0.15
0.12
0.09
0.06
0.03
0.00
^{14}C-Albumin Flux (pmol/h)
Baseline
Media
LPS(10 ng/ml)
LPS+ENP(100 ng/ml)
*
Baseline
Media
Escherichia coli 0111:B4
Escherichia coli 055:B5
Pseudomonas aeruginosa
Klebsiella pneumoniae
Serratia marcescens
Salmonella minnesota
n = 69
9
4 6
4 6
4 6
4 6
4 6
4 6

Fig 15

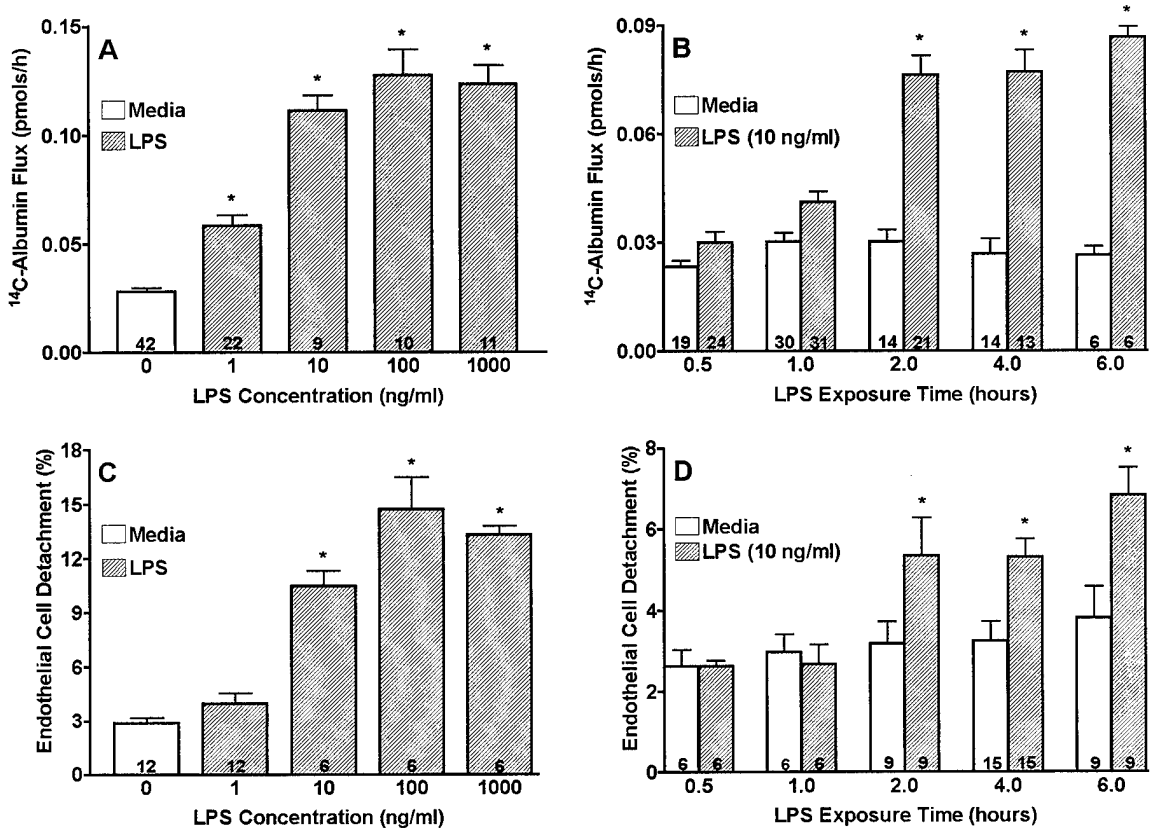
A
Media
LPS
^{14}C-Albumin Flux (pmols/h)
0.15
0.10
0.05
0.00
42
22
9
10
11
0
1
10
100
1000
LPS Concentration (ng/ml)
B
Media
LPS (10 ng/ml)
^{14}C-Albumin Flux (pmols/h)
0.09
0.06
0.03
0.00
19
24
30
31
14
21
14
13
6
6
0.5
1.0
2.0
4.0
6.0
LPS Exposure Time (hours)
C
Media
LPS
Endothelial Cell Detachment (%)
18
15
12
9
6
3
0
12
12
6
6
6
0
1
10
100
1000
LPS Concentration (ng/ml)
D
Media
LPS (10 ng/ml)
Endothelial Cell Detachment (%)
8
6
4
2
0
6
6
6
6
9
9
15
15
9
9
0.5
1.0
2.0
4.0
6.0
LPS Exposure Time (hours)

Fig 16

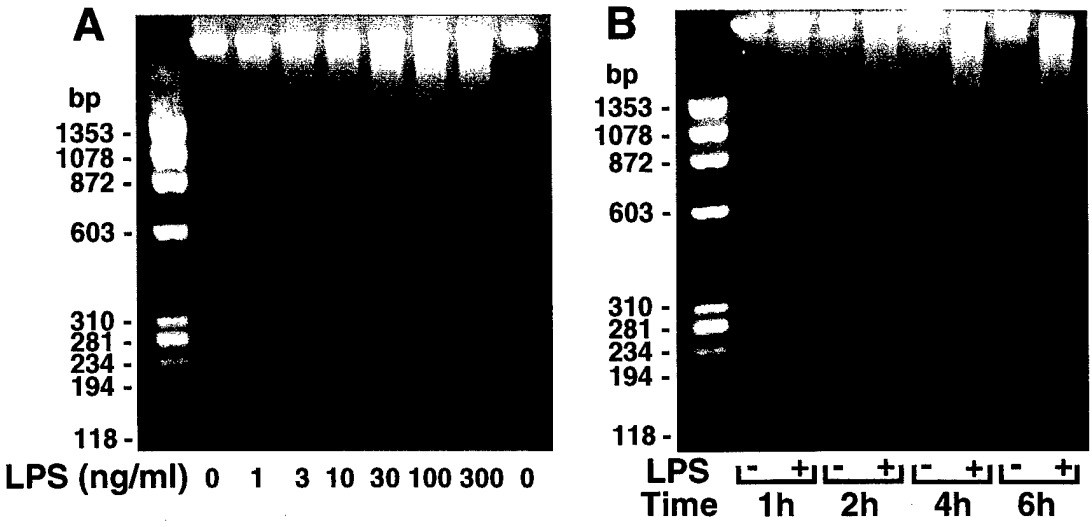
A
bp
1353 -
1078 -
872 -
603 -
310 -
281 -
234 -
194 -
118 -
LPS (ng/ml) 0 1 3 10 30 100 300 0
B
bp
1353 -
1078 -
872 -
603 -
310 -
281 -
234 -
194 -
118 -
LPS - + - + - + - +
Time 1h 2h 4h 6h

Fig 17

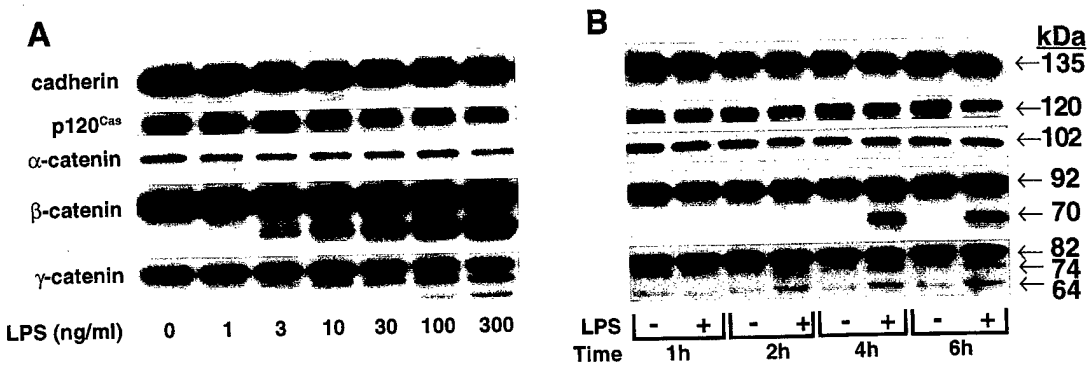
A
cadherin
p120Cas
α-catenin
β-catenin
γ-catenin
LPS (ng/ml) 0 1 3 10 30 100 300
B
kDa
←135
←120
←102
← 92
← 70
← 82
← 74
← 64
LPS - + - + - + - +
Time 1h 2h 4h 6h

Fig 18

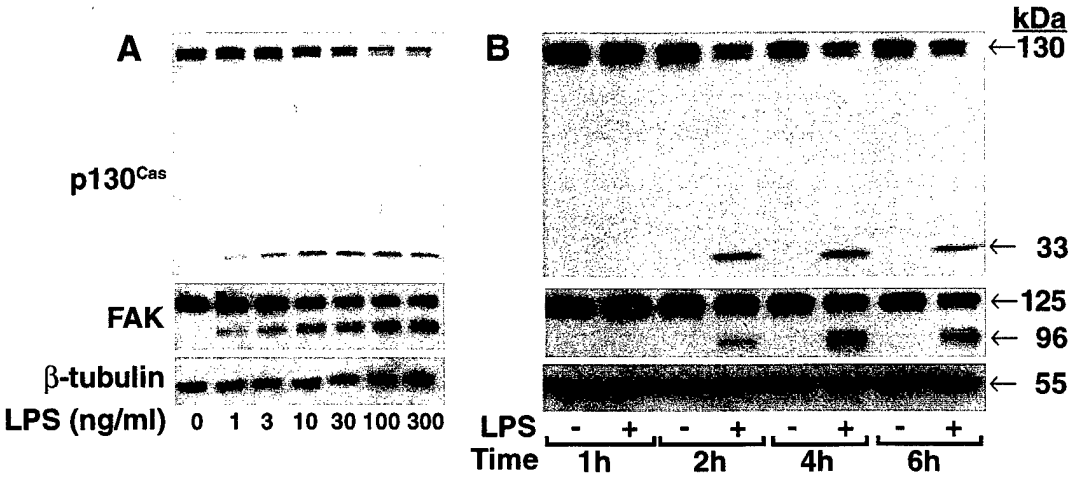
A
p130Cas
FAK
β-tubulin
LPS (ng/ml) 0 1 3 10 30 100 300
B
kDa
←130
← 33
←125
← 96
← 55
LPS - + - + - + - +
Time 1h 2h 4h 6h

Fig 19

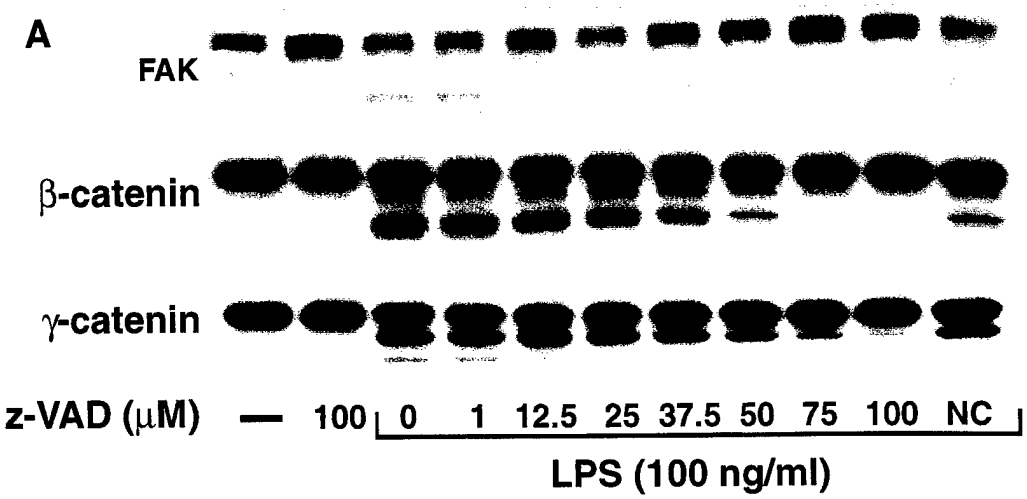
A
FAK
β-catenin
γ-catenin
z-VAD (μM) — 100 0 1 12.5 25 37.5 50 75 100 NC
LPS (100 ng/ml)

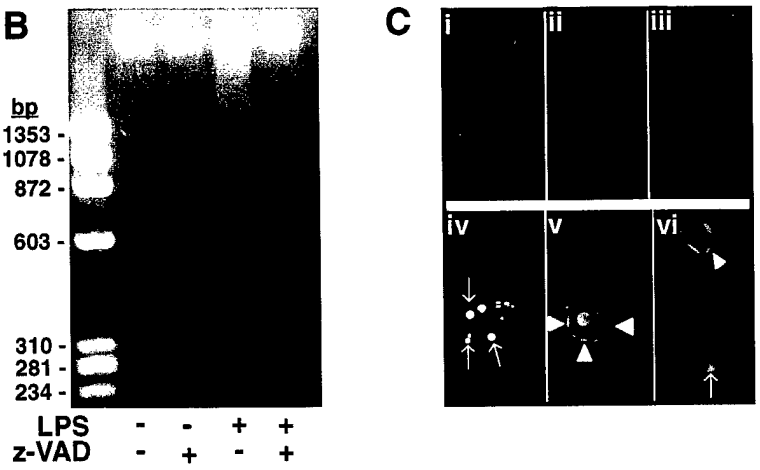
B
bp
1353
1078
872
603
310
281
234
LPS - - + +
z-VAD - + - +
C
i
ii
iii
iv
v
vi

Fig 20

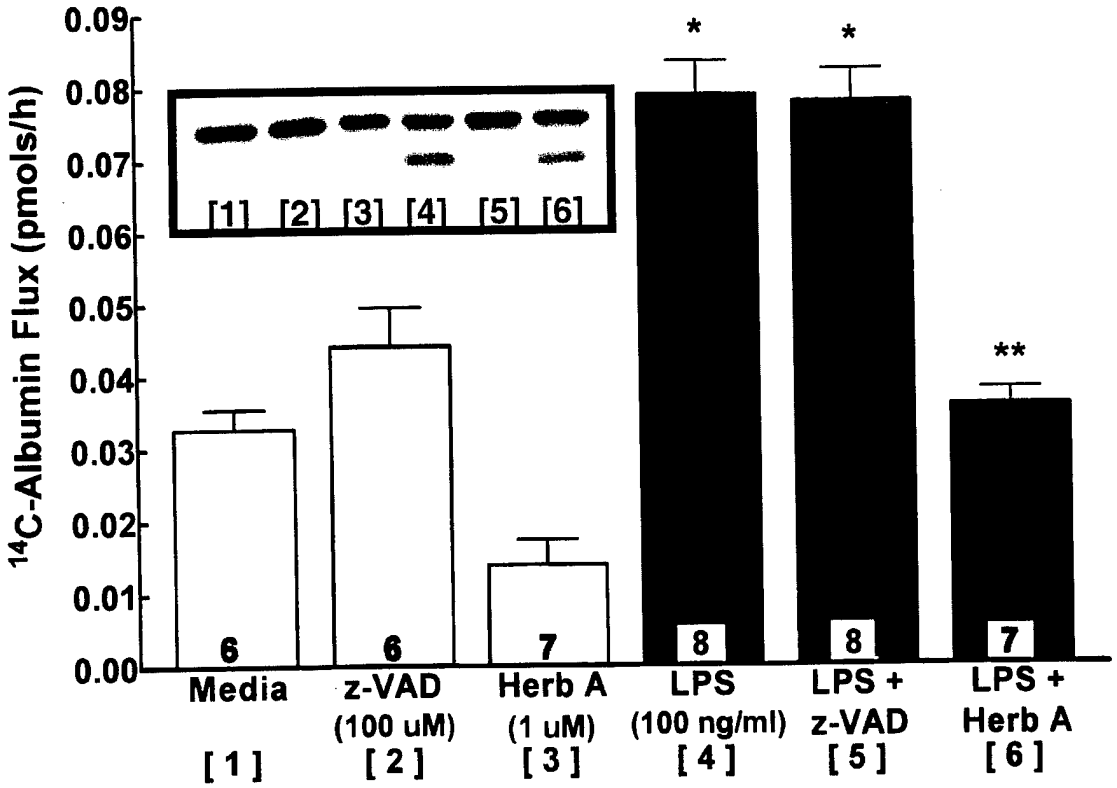
0.09
0.08
0.07
0.06
0.05
0.04
0.03
0.02
0.01
0.00
14C-Albumin Flux (pmols/h)
[1] [2] [3] [4] [5] [6]
*
*
**
6
6
7
8
8
7
Media
[1]
z-VAD
(100 uM)
[2]
Herb A
(1 uM)
[3]
LPS
(100 ng/ml)
[4]
LPS +
z-VAD
[5]
LPS +
Herb A
[6]

Fig 21

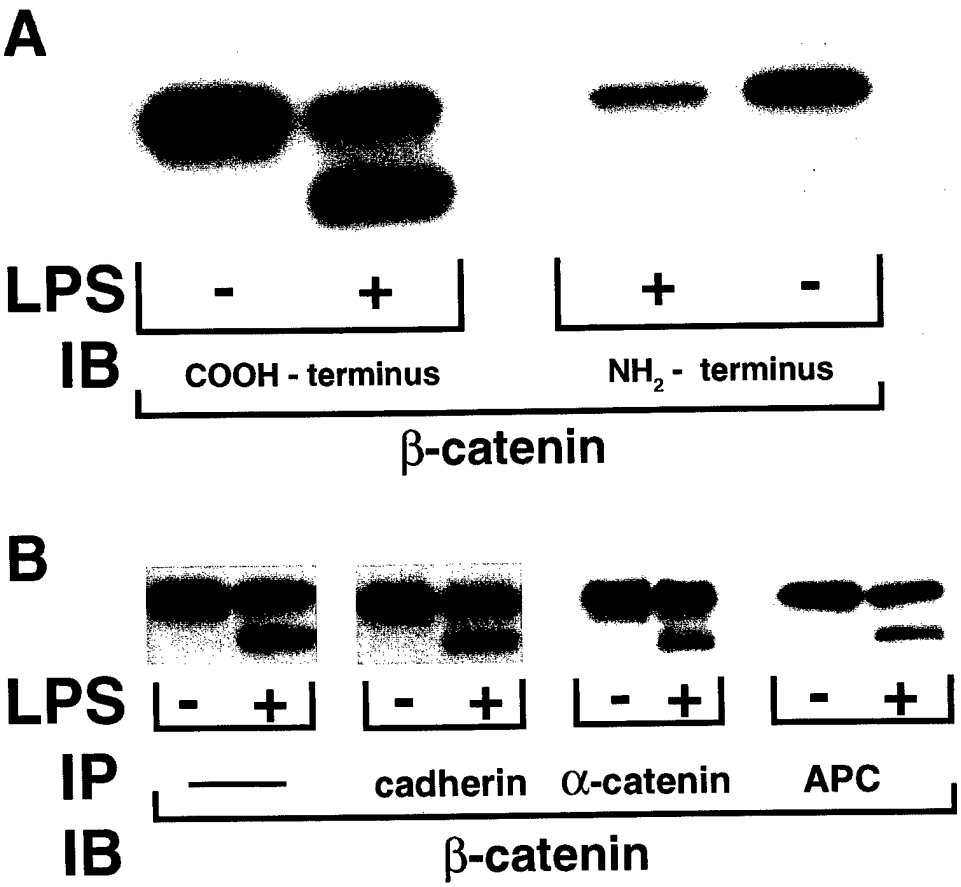
A
LPS
- +
+ -
IB
COOH - terminus
NH2 - terminus
β-catenin
B
LPS
- + - + - + - +
IP
cadherin
α-catenin
APC
IB
β-catenin

Fig 22

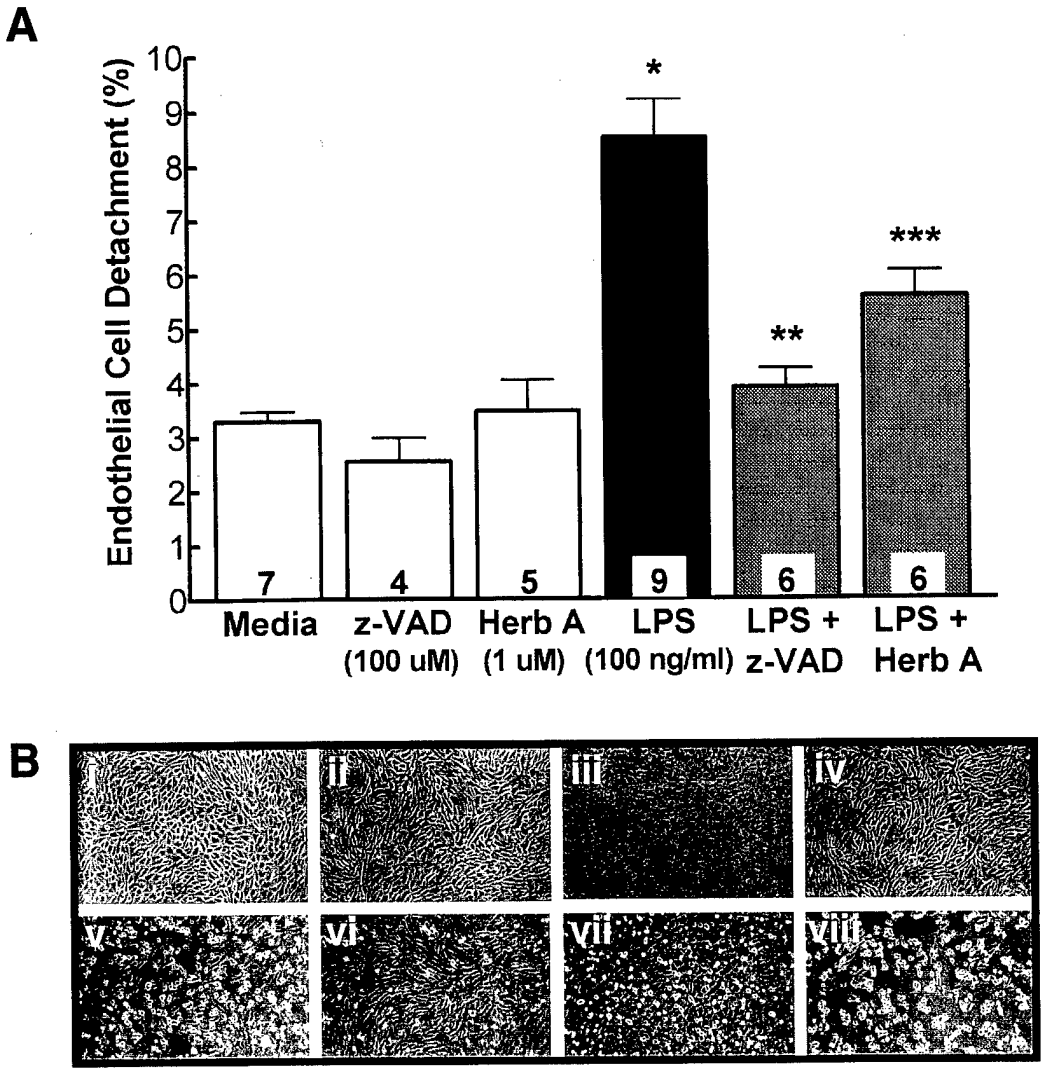
A
Endothelial Cell Detachment (%)
10
9
8
7
6
5
4
3
2
1
0
*
**
***
7
4
5
9
6
6
Media
z-VAD (100 uM)
Herb A (1 uM)
LPS (100 ng/ml)
LPS + z-VAD
LPS + Herb A
B
i
ii
iii
iv
v
vi
vii
viii

Fig 23

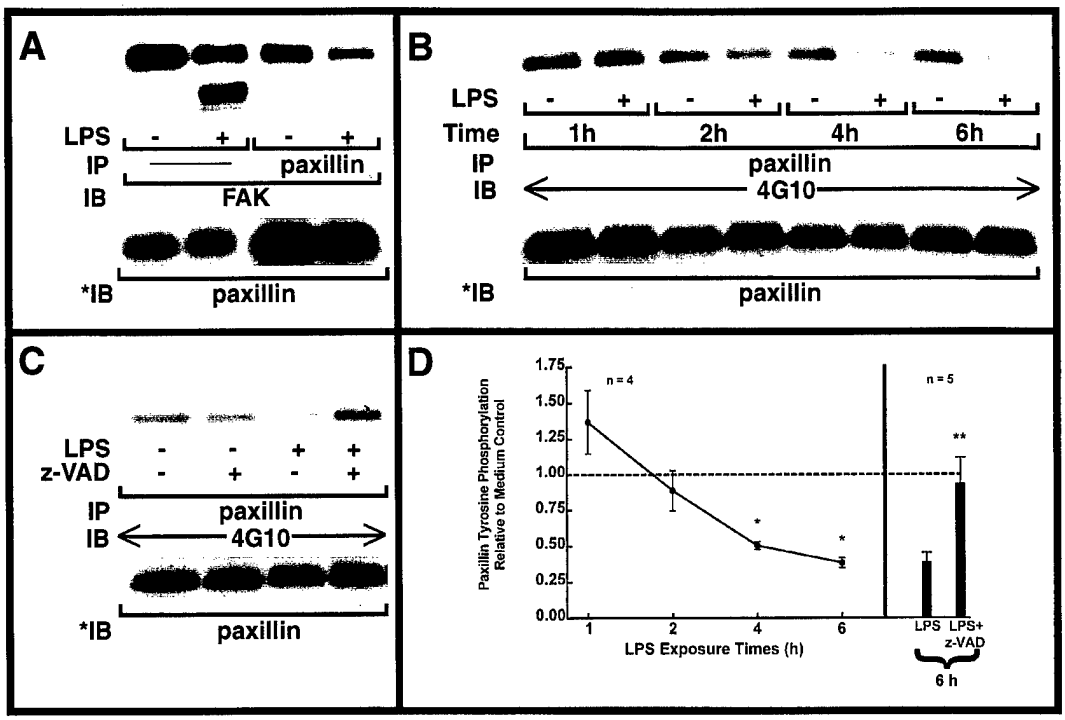
A
LPS
IP
IB
paxillin
FAK
*IB
paxillin
B
LPS
Time
1h
2h
4h
6h
IP
paxillin
IB
4G10
*IB
paxillin
C
LPS
z-VAD
IP
paxillin
IB
4G10
*IB
paxillin
D
Paxillin Tyrosine Phosphorylation Relative to Medium Control
n = 4
n = 5
LPS Exposure Times (h)
LPS
LPS+ z-VAD
6 h

Fig 24

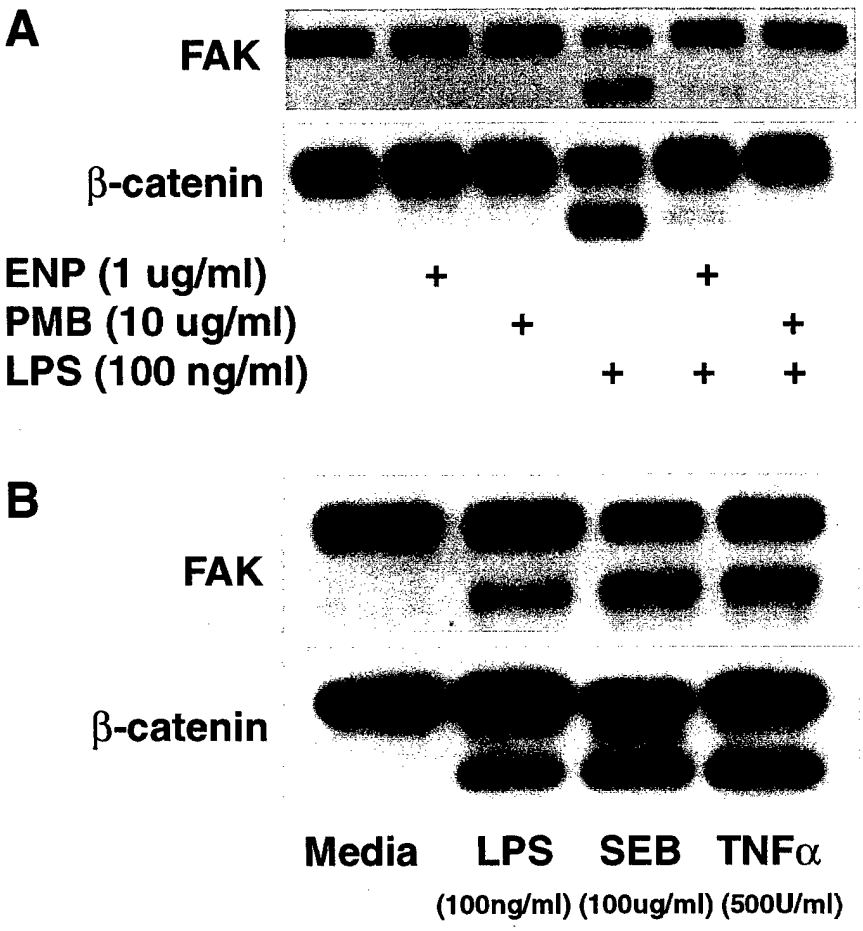
A
FAK
β-catenin
ENP (1 ug/ml) + +
PMB (10 ug/ml) + +
LPS (100 ng/ml) + + +
B
FAK
β-catenin
Media
LPS (100ng/ml)
SEB (100ug/ml)
TNFα (500U/ml)

Fig 25

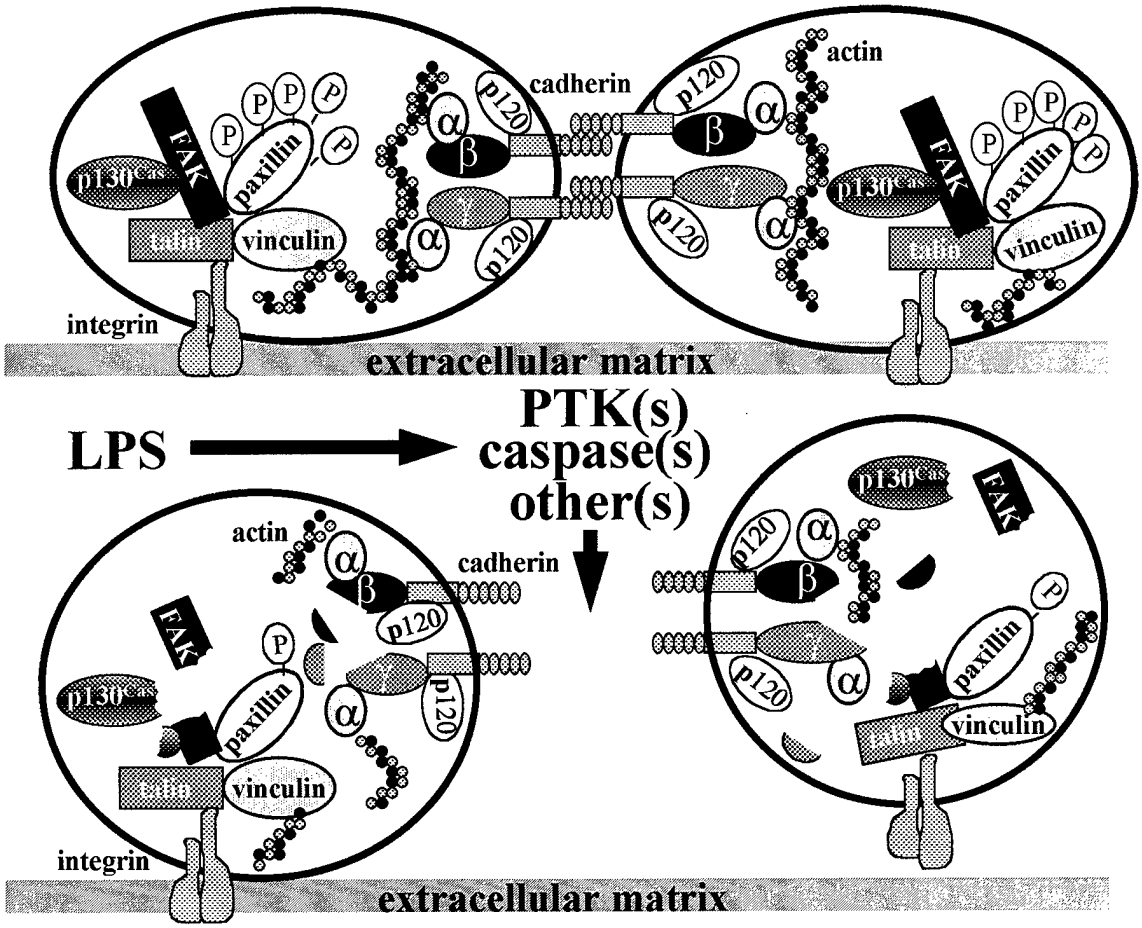
cadherin
actin
FAK
paxillin
p130Cas
talin
vinculin
integrin
extracellular matrix
p120
LPS
PTK(s)
caspase(s)
other(s)

Fig 26